Single-molecule conductance measurements in mechanically controlled break junctions

Determining the conductance of two porphyrins and spiropyran

L.F. de Niet

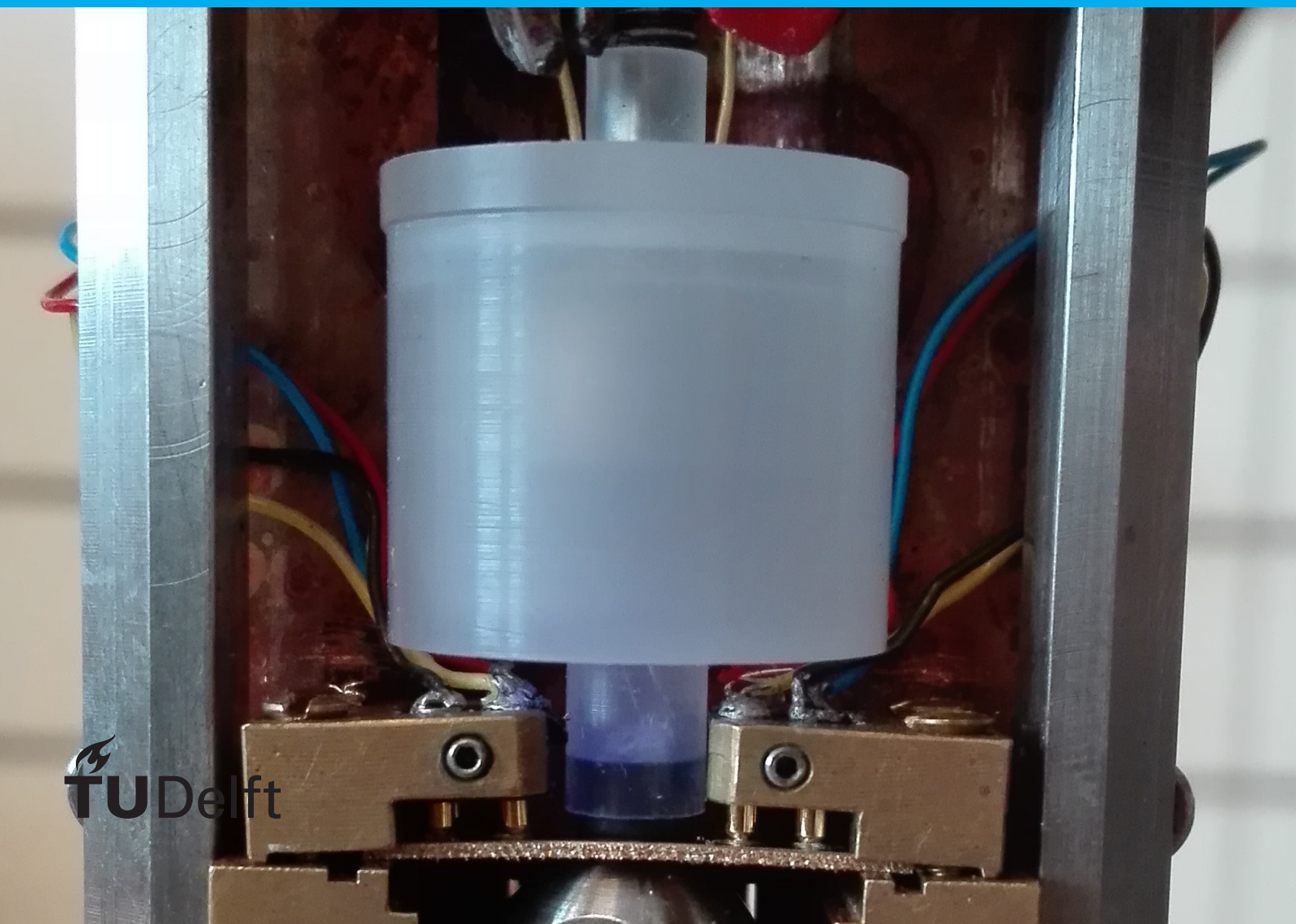

Single-molecule conductance measurements in mechanically controlled break junctions

Determining the conductance of two porphyrins and spiropyran

by

L.F. de Niet

to obtain the degree of Master of Science
at the Delft University of Technology,
to be defended publicly on 23 August 2018.

Student number:	4139658	
Project duration:	December 1, 2017 – August 23, 2018	
Thesis committee:	Prof. dr. ir. H.S.J. van der Zant,	TU Delft, supervisor
	Prof. dr. Y.M. Blanter,	TU Delft
	Dr. F.C. Grozema,	TU Delft

TU Delft

Preface

Here in front of you lies my thesis with the title "Single-molecule conductance measurements in mechanically controlled break junctions". This thesis is the final hurdle to earn my master degree in Applied Physics. Physics was not a choice I made at the end of high school. Ever since I was young I wanted to know how things worked in the world around me. It started with biting in things and throwing them away and seeing what would happen. Over the years the biting and throwing have slowly been replaced with a more systematic approach of interacting with objects around me. In high school physics classes I learned formulas that would allow me to predict my interaction with nature and I could check those predictions with experiments. And with these predictions I was able to shape the world around me and fabricate machines to do my bidding. This feeling of being the master of my ennvironment did not last long. As soon as I entered the bachelor in Delft my world was turned upside down. Everything I thought I knew had to be put in a different perspective. The world around me was not so simple as I assumed. I was just lucky that my bike, a car or a marble are, in a physical sense, slow and big objects. In my bachelor I was introduced to the miraculous world of quantum mechanics. Just keep zooming in on regular objects and the laws of physics will break down and have to be replaced with a new set of rules to govern the behaviour of particles. But this behaviour was not as straightforward as kicking a ball or shooting a marble. If I kick a ball ten times in an identical way, it will end up on the same place each time. But in this new world this would not necessarily be the case. And during my master I encountered even more bizarre effects. The strange world of quantum mechanics keep me fascinated to this very day. But I was determined to also use this physics to shape the world around me and manipulate it in a predictable way. So my master thesis is really a logical next step in my journey through physics. In this work I use the laws of the very tiny to try to create a very tiny machine.

I hope you will enjoy reading this thesis.

L.F. de Niet
Delft, August 2018

Contents

1

Introduction

1.1. Molecular electronics

Molecular electronics is the field that studies the use of molecules as building blocks for new electronic components. The research focusses on both the application and the underlying physics of these components. In the last thirty years, a lot of progress has been made in the field, but there are still many (fundemental) questions to be answered. The start of molecular elecronics is usually associated with the paper by Aviram and Ratner on the design of a molecular diode [2]. In this paper, a rectifier is described based on a single molecule. This molecule could not be measured in those days, because the experimental techniques to do so were not present. It took approximately twenty years to reliably measure single molecules in a scanning tunneling microscope and a few more years for the development of break junction set-ups. In current experiments single-molecule measurements are possible and large amounts of data can be gathered relatively fast.

1.2. Thesis outline

This thesis consists of two main parts. The first part is a review of the relevant literature on single-molecule photoswitches. The second part consists of practical work done in the van der Zant lab. In this practical work, three different molecules were measured.

In chapter 2 the reader will be provided with the theoretical framework to understand the physics of charge transport in molecular juntions.

Chapter 3 contains a description of the set-up employed for the measurements and the experimental methods. Along with data aquisition, this chapter also introduces ways display and interpet the data. In this work the set-up was adapted to allow a new type of measurement. A description of the adapted set-up and a corresponding measurement protocol is included in this chapter.

The review of the relevant single-molecule photoswitch literature can be found in chapter 4. Multi-molecule measurements are also included in the review, but not as extensively as single-molecule experiments. This chapter provides the reader with an insight into the experimental progress in the field of molecular photoswitches so far.

The conductance measurements of two new porphyrin molecules are discussed in chapter 5. The results of one of the porphyrin measurements are compared with previously done OPE-3 measurements to gain insight in the relation between molecular conductance and yield.

Chapter 6 details the measurements on the photoswitchable molecule spiropyran. In this chapter the influence of light on the conductance of the molecule is subject of research.

2

Charge Transport in Molecules

In order to describe current through molecules, Ohm's law cannot be used. Ohm's law is a macroscopic description of the average movement of electrons. In the classical Drude model, electrons are accelerated by an electric field. These electrons move through the material until they scatter. The average distance an electron travels between two impacts is the mean free path. Because the scale of household electronics is much larger than the mean free path, the number of electrons and collisions is big enough to describe the net current with Ohm's law. When the scale of the device comes near or gets below the mean free path, Ohm's law fails. A way to describe charge transport in this situation will be discussed in this chapter. First, the behaviour of electrons in uncoupled molecules will be discussed and then that of a molecule coupled to two leads. This chapter will only touch on the subject briefly, a full description of the theory can be found in the literature [44][33][7].

2.1. Orbitals

Charge transport is the transport of electrons or holes. Electrons in molecules occupy orbitals. Each orbital has a fixed energy and can be occupied by at most two electrons because of the Pauli exclusion principle. The simplest example is an electron in a single hydrogen atom. This case is treated in every quantum mechanics course. In big molecules the orbitals are more difficult to calculate, but they still are discrete levels with a fixed energy. Not all orbitals of a molecule are filled. Two orbitals are of special interest: the highest occupied molecular orbital (HOMO) and the lowest unoccupied molecular orbital (LUMO). Either of these orbitals can be responsible for charge transport in the single-level model. The HOMO is responsible for hole transport and the LUMO for electron transport.

2.2. Single-level model

The basis of the single-level model is a nano object connected to two leads. The object has discrete levels, in the case of molecules these are orbitals, and these levels can be used as transport channels for charges. A schematic of this model can be seen in figure 2.1. On the left three levels are visible. The single-level model of this junction can be seen on the right. The single-level model assumes the energy levels of the scatterer are far apart and one level is close to the Fermi energy. In this case the transport will be dominated by the level closest to the Fermi energy. Only this level is taken into account and the other levels are neglected. The coupling of this level to the source and drain is indicated with Γ_S and Γ_D respectively. In figure 2.1 the current is blocked, if a bias is applied a current will start to flow when the single-level is inside the bias window.

When a molecule is connected to one or more electrodes, the molecular properties change. As a result of metal-molecule coupling, the molecular orbitals hybridize with the states of the metal contacts. This results in a broadening and shift in the molecular levels. The description and prediction of this shift and broadening is an ongoing subject of research. Another way to look at this is with the Heisenberg uncertainty principle. If a molecule is not connected to any leads, the electron stays on the molecule for a very long time and the variation in energy is very small. But when the time spent on the molecule is small, in case of transport, the variation in energy increases. For one level, the resulting molecular density of states $D(E)$ is given by a Lorentzian:

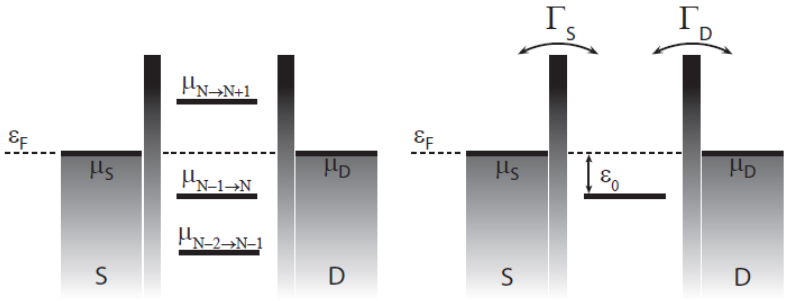

Figure 2.1: The single-level model. On the left the system we want to model and on the right the single-level model. The single-level model only deals with the level closest to the Fermi energy. Adapted from [34].

$$D(E) = \frac{1}{2\pi} \frac{\Gamma}{(E - E_0)^2 + (\Gamma/2)^2}, \tag{2.1}$$

where E_0 is the energy of the modified orbital. The total broadening is the sum of the coupling to each of the electrodes Γ_S and Γ_D, so $\Gamma = \Gamma_S + \Gamma_D$.

2.3. Transport regimes

To determine which transport mechanism is responsible for the charge transport, one has to look at the energy scales of the system. These energies are the thermal energy $k_B T$, the coupling energy Γ and the charging energy U. In the case of weak coupling, $U \gg \Gamma, k_B T$, the junction behaves as a Coulomb blockaded system [33]. The electrons tunnel through the molecule one by one. An extra electron can be added if the energy barrier U is overcome. In this regime, the number of electrons on the molecule are integers and the transport can be descibed by a master equation formalism. In the case of strong coupling, $\Gamma \gg U$, the electron transport is coherent and the number of electrons on the molecule is not well defined. To first order, the current through one level van be calculated using the Landauer formula

$$I(V) = \frac{G_0}{e} \int_{-\infty}^{\infty} T(E) \left[f_S(E) - f_D(E) \right] \, \mathrm{d}E, \tag{2.2}$$

where $f(E)$ is the Fermi-Dirac distribution of the left and the right lead respectivly and $T(E)$ is the transmission function given by

$$T(E) = 2\pi \frac{\Gamma_S \Gamma_D}{\Gamma_S + \Gamma_D} D(E) = \frac{\Gamma_S \Gamma_D}{(E - E_0)^2 + (\Gamma/2)^2}. \tag{2.3}$$

If we solve integral 2.2 for a single level at zero temperature with symmetric barriers, we find an analytical expression for the current as a function of the symmetric applied bias:

$$I(V) = \frac{G_0}{e} \Gamma \left[\arctan\left(2 \frac{eV - E_0}{\Gamma} \right) - \arctan\left(2 \frac{-eV - E_0}{\Gamma} \right) \right]. \tag{2.4}$$

3

Experimental Set-up and Data Representation

This chapter contains a description of the measurement set-up and the data aquisition protocols. The mechanically controlled break junction (MCBJ) is used to measure single-molecule conductances. Various ways of displaying and interpreting the data are introduced as well. Then, data selection is covered and this chapter ends with a description of the illuminated liquid cell, the new measurement protocol and alternative measurements.

3.1. MCBJ set-up

In this work all measurements are done with an MCBJ. The set-up and sample fabrication are described in great detail in other works [29]. This thesis will only contain a short outline of the measurement set-up. The illuminated liquid cell will be discussed in greater detail, because it was added to the set-up as a part of the thesis work.

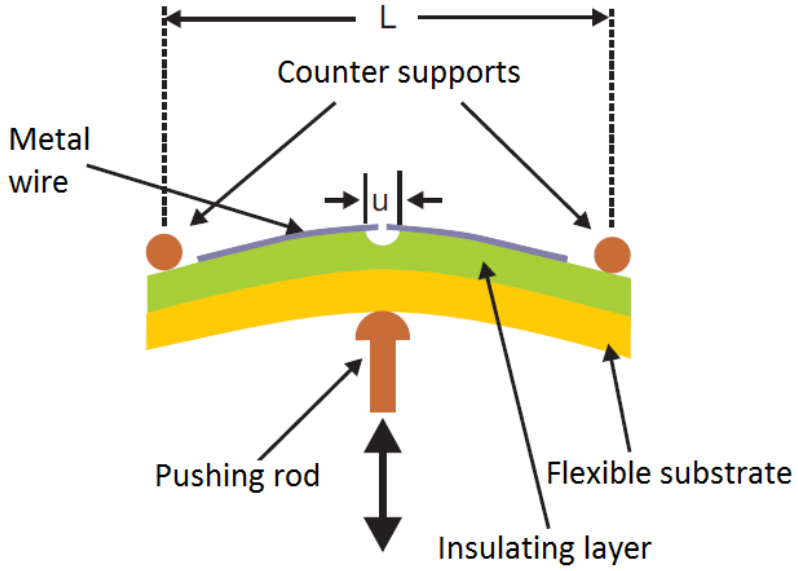

Figure 3.1: A schematic representation of a mechanically controlable break junction set-up. Adapted from [7].

The MCBJ is a popular and widely used device to measure single-molecule conductance. In an MCBJ measurement, a golden wire with a constriction is placed on a flexible substrate. Pressure is applied to the substrate with a piezo element to bend it. The bending of the substrate streches the wire, first it becomes a

single point contact and then it breaks completely, forming a nanogap. If molecules are present around the constriction, a molecule can form a bridge between the two parts of the golden wire. The junction is restored by releasing the applied pressure on the substrate. The exact configuration of the junction is unknown in MCBJ measurements. Every time the wire is broken other atoms may be the last to break, molecules may or may not be present inside the junction and the molecular configuration may differ. Despite this drawback the MCBJ is a widely used tool because, since the junction can be broken and made repeatedly, it is possible to collect data on thousands of junctions, which allows for statistical analysis of the junctions and the molecules inside them. Another advantage of the MCBJ is the possibility to do measurements in different environments. The measurements can be done in ambient conditions, but also in vacuum, and the set-up can be operated at room temperature or be cooled down to cryogenic temperatures.

3.2. Breaking traces

The way information is gathered from the junction is by collecting so-called breaking traces. The conductance of the junction is measured while the substrate is being bent. A potential difference is applied to the junction and the current is measured as a function of piezo voltage. From this data the conductance versus displacement plots are made. Typical voltages at room temperature range between 50 mV and 250 mV. An example of these breaking traces can be seen in figure 3.2.

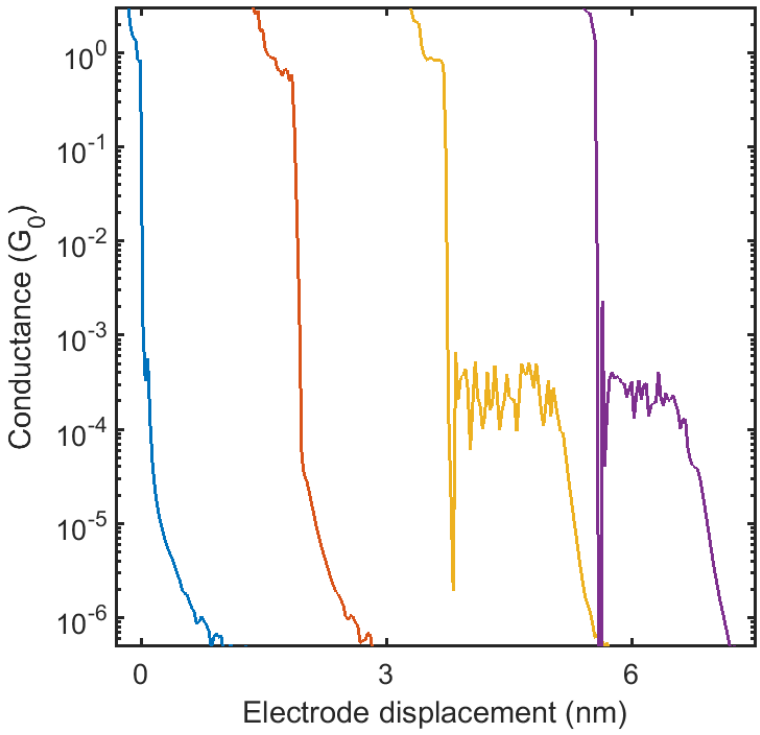

Figure 3.2: Four examples of breaking traces. The first two traces are without a molecule between the electrodes and the last two are with a molecule inside the nanogap.

This figure shows two traces with and two traces without a molecule present. The conductance decreases in steps to 1 G_0 $\left(=\frac{2e^2}{h} \approx 7.748 \cdot 10^{-5}\ \mathrm{S}\right)$ corresponding to the formation of a gold chain, because gold atoms have only one fully transmitting channel. Upon further streching the point contact breaks and the gold electrodes relax inducing a drop in conductance of three to four orders of magnitude. This relaxation is called snapback and forms a gap around 0.5 nm [54]. After this snapback the substrate is bent even more and the current drops exponentially. If there is no contact between the two electrodes the electrons can only tunnel to the other side and the chance of tunneling depends on the distance exponentially. These traces without a molecule are called tunneling traces. When there is a molecule present between the electrodes, the trace shows different behaviour. After breaking the single point contact between the two electrodes, a molecule can

bridge the gap. In that case the current can pass through the molecule. The yellow and purple trace in figure 3.2 show molecular traces. The horizontal plateau around $2 \cdot 10^{-4}$ G_0 indicates the presence of a molecule. After further bending, the molecular junction breaks and the conductance drops exponentially again. After each trace the junction is fused back to 50 G_0 to ensure atomic rearrangement of the golden wire.

The junction can not be broken and made indefinitely. After breaking many times, usually more than several thousand times, the junction breaks down and cannot be used anymore. In this case the junction can not be broken or made completely anymore. In this case the measurement is stoppend and the data is selcted in such a way as not to include the faulty traces in the data analysis.

3.3. Data respresentation

The gathered data can be presented in several ways. The most common are the one-dimensional and two-dimensional histograms. To create the 1D histogram, the conductance axis is divided in bins and the number of datapoints inside each bin of every traces is counted and summed up. For the 2D histogram the traces have to be aligned to a reference zero displacement. This is done at the rupture of the 1 G_0 plateau. Next the conductance and the displacement axis are binned and the datapoints inside each bin are counted for all traces again. A bare gold and molecular example of these plots can be seen in figure 3.3.

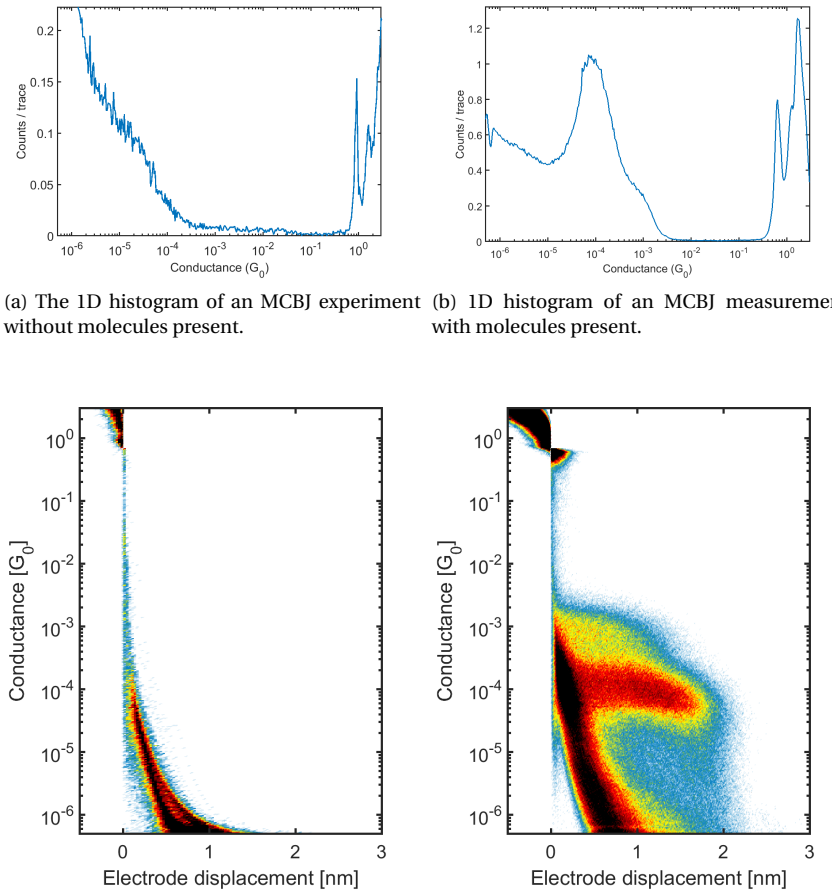

(a) The 1D histogram of an MCBJ experiment without molecules present.

(b) 1D histogram of an MCBJ measurement with molecules present.

(c) 2D histogram of an MCBJ measurement without molecules present.

(d) 2D histogram of a molecular measurement.

Figure 3.3: 1D and 2D histograms of an empty gold measurement and a molecular measurement.

Both the 1D histograms in figure 3.3 show a clear peak at 1 G_0. This indicates the junction often forms a single gold contact before breaking. In figure 3.3a there are almost no counts between 1 G_0 and 10^{-4} G_0 because of the snapback. Below 10^{-4} G_0 the tunneling counts appear in both the 1D histograms. Around 10^{-7} G_0 the 1D histograms have a large peak. This peak is the noisefloor of the set-up. The molecular histograms differ clearly from the tunneling histograms. The molecular 1D histogram in figure 3.3b shows two

peaks between 10^{-5} G_0 and 10^{-2} G_0. These two peaks correspond to the two plateaus visible in the 2D histogram in figure 3.3d. Fitting the 1D histogram gives us the most probable conductance value of a molecule. In a molecular measurement there can also be tunneling traces present, as can be seen in figure 3.3d. The yield of a measurement is the number of molecular traces divided by the total number of traces. The yield depends on the number of molecules near the junction. But if the chance of trapping a molecule is large, there is also a fair chance of trapping multiple molecules simultaneously. The focus of this work is on single-molecule conductance measurements, so the yield should be large enough to gather enough data for a statistical analysis of the traces, but small enough to ensure that the chance of trapping multiple molecules in a junction is low.

3.4. Sorting the traces

During the analysis of the data, it is useful to filter or sort the data. By filtering the molecular traces from the tunneling traces the yield can be determined. Two filters are used in this work. The first filter is the so called "slope filter". This filter takes two inputs: a length and a slope. The filter then checks if the slope of a trace is higher or lower than the set slope for a set length. An example of this filter can be seen in figure 3.4a. This figure and the inset both display a purple line. All traces with a higher slope than this line between 0.3 nm and 0.7 nm are selected and traces with a lower slope are discarded. The main figure shows the 2D histogram of the selected traces and the inset shows the 2D histogram of the discarded traces.The second filter is the "window filter". This filter counts the number of datapoints in a certain conductance window for each trace and determines the average number of counts in that window. A trace is selected if the number of counts is more than C times the average. Uncareful selection of the window and the constant C can produce misleading results. If the window is chosen shallow and C is large, the resulting 1D histogram will always show a peak in the chosen window. This can be seen in figure 3.4b. The 1D histograms in this figure are the results of the window filter on the measurement seen in figure 3.3c. The 1D histogram of the selected traces show an increase in counts between $2 \cdot 10^{-3}$ G_0 and $2 \cdot 10^{-2}$ G_0. It is wise to use a wide window and a moderate C.

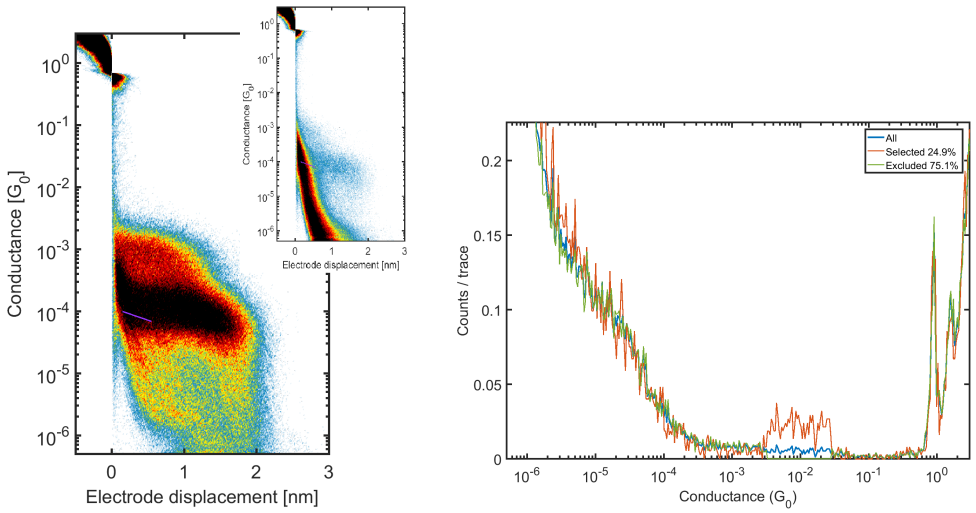

(a) The 2D histogram of the traces selected by the slope filter. The inset shows the discarded traces.

(b) The window filter applied on measurement without molecules. The 1D histogram of the selected traces show a peak around 10^{-2} G_0.

Figure 3.4: An example of each filter. Figure (a) shows the result of the slope filter on the molecular measurement seen in figure 3.3d and figure (b) shows the result of the window filter on the gold measurement seen in figure 3.3c.

The third way to sort the traces used in this work is the clustering method. This method starts the same way as the fabrication of the 2D histogram. A grid is placed over the trace and the datapoints on each face are counted. This grid of counts is transformed into a vector that represents a point in the so-called image space. Traces with similar features will lay close together in this image space. A k-means algorithm clusters the point in a predefined number of classes. This algorithm divides the points in sets in such a way as to minimize the variance within all the sets. First the centroids of the classes are initialized using a k-means++ algorithm. This

algorithm picks the first centroid randomly as one of the traces in image space. Next the algorithm calculates the distance of all other points in image space to the nearest centroid. Then the algorithm chooses a datapoint as new centroid with a probability proportional to the square of the distance to the nearest centroid. This calculation of the distance to the nearest centroid and the random assingment of centroid continues until all centroids are initialized. Now the k-means algorithm starts to cluster the traces. At each iteration the points in the image space are assinged to the nearest centroid. The centroid is then updated to the mean of all the assinged traces. This process continues until the clustering is converged and the points do not change cluster upon iteration anymore. The k-means algorithm does not necessarily produce the optimal clustering. The result of the algorithm depends on the initialization of the centroids. The k-means++ initialization is used because it produces relatively good solutions [3]. Also, the clustering is done ten times and the solution with the lowest total variance is chosen as the final result. With this method it is possible to group traces with similar features together.

3.5. Molecular deposition

In this work there are two methods were employed to deposit the molecule on the junction: dropcasting and the liquid cell. In both cases the molecule of interest is dissolved in an organic solvent. This solution is dropcasted onto the junction with a syringe. The volatile solvent evaporates and the molecule is left on the junction. Another way of getting the molecules near the junction is with the use of a liquid cell. The liquid cell used is a teflon funnel that can be placed over the metallic junctions. At the bottom of the funnel a viton ring is placed to ensure the solution stays inside the funnel and can not leak out into the set-up. The molecule is dissolved in a solvent and injected into the liquid cell. The solution in the liquid cell has to be chosen such that it does not show up in the measurements. To check this the solvents are measured in the liquid cell without the molecule. The way to deposit the molecule onto the junction depends on the type of measurement and the properties of the molecule.

3.6. Illumated liquid cell

This thesis contains measurements to determine the influence of light on the molecular conductance in an MCBJ set-up. During these measurements the molecule will be inserted in a liquid cell. The present liquid cell did not allow for an LED to be present during the measurements, so the liquid cell was adapted. In the new liquid cell the LED shines directly onto the junctions, so the light interacts with the molecules close to the junction. If the LED is misaligned the effect of the light on the conductance can wear off in the time it takes for the molecule to diffuse to the junction and be measured. So the LED has to be placed inside the liquid cell and shine right on the junction. To place the LED directly above the samples, two extra holes were added to the lid of the cell. The new lid can be seen in figure 3.5. The big hole was already present in the old lid and is used to inject the solution into the liquid cell. The two small holes on both sides of the top are added to the design and are just wide enough to fit the anode and cathode of the LED. This lid allows us to place the LED right above the sample and face it direclty at the junctions.

Before the new illuminated liquid cell could be used for measurements, the cell had to be tested. Because the LED is present inside the cell, the rubber ring that is normally added to minimize evaporation can not be placed inside the cell. There are also two more holes in the lid and because the LED takes space inside the cell, less solution can be injected inside the cell. The test will show how long the solution can stay inside the illuminated liquid cell and check for other unexpected side effects of the LED. The illuminated liquid cell inside the MCBJ set-up can be seen in figure 3.6 with the LED on and off. The light of the LED is indeed pointed towards the sample and reaches the junctions directly.

The tests of the liquid cell showed that the solution stays inside the cell for more than 48 hours. Even with the extra holes, without the rubber seal and the reduced amount of solution. After this time a single droplet can be added to ensure the presence of solution for another day. The junctions inside the liquid cell can be broken thousands of times, just like in ambient conditions. These results make the illuminated liquid cell a valuable tool in the research of molecular conductances in an MCBJ.

3.7. Illuminated MCBJ measurements protocol

Some measurements in this thesis investigate the influence of light on the molecular conductance. This is done by collecting breaking traces with the LED on and off. The LED is switched on and off every 500 traces. During all these traces the applied bias and the breaking speed is kept constant. The number of traces

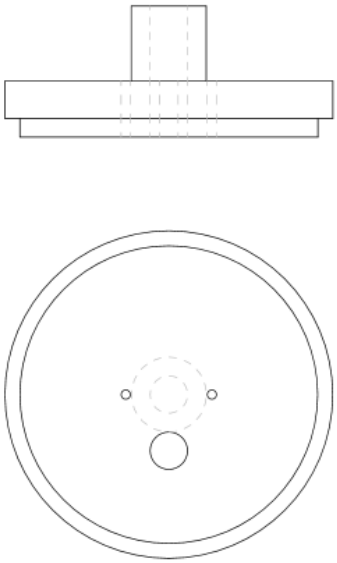

Figure 3.5: The lid of the illuminated liquid cell. On the top, the side view of the lid and below the bottom view of the lid. The big hole is used to inject the solution and the two small holes are used to wire the LED.

between switching events is a balance between different needs. Less frequent switching means there are more traces to analyze between switching events, but if an external factor, like temperature, influences the measurements, less frequent switching induces a loss of temperature resolution.

3.8. Real-time photoswitching

It is possible to measure the influence of light on the conductance in another way with an MCBJ. If the molecule of interest is a photoswitch, a molecule that changes it structure upon irradiation, other measurements are possible. Instead of switching the molecule in the solution and measure its conductance, the molecule can be captured and then switched while it is being measured. Figure 3.7 shows a possible realisation of such a measurement. The molecule is trapped between the electrodes and is kept there for a few seconds. The LED is switched on between the two dotted lines. After some time in the light, the molecule switches. This switching causes the LED to turn off. After the relaxation time of the molecule it returns to the high conductance state. This measurement allows one to measure the conductance of each state and the relaxation time of a molecular photoswitch. To preform this measurement, the molecule and set-up have to meet some demands. The molecule has to be able to switch when connected to the leads and the switching has to cause a change in conductance large enough to reliably be measured, so at least one order of magnitude. Next, the lifetime of the switched state has to be long enough to measure but short enough to preform multiple switiching events before the junction breaks; between 0.1 s and 10 s. This also requires the lifetime of the junction to be in the order of minutes. In the example the molecule switches back by thermal relaxation, but if the molecule can switch back upon irradiation with another wavelength, a different LED could also be used. These measurements can be done inside the liquid cell, but also in ambient conditions. The exact details of the measurement depend on the characteristics of the molecule.

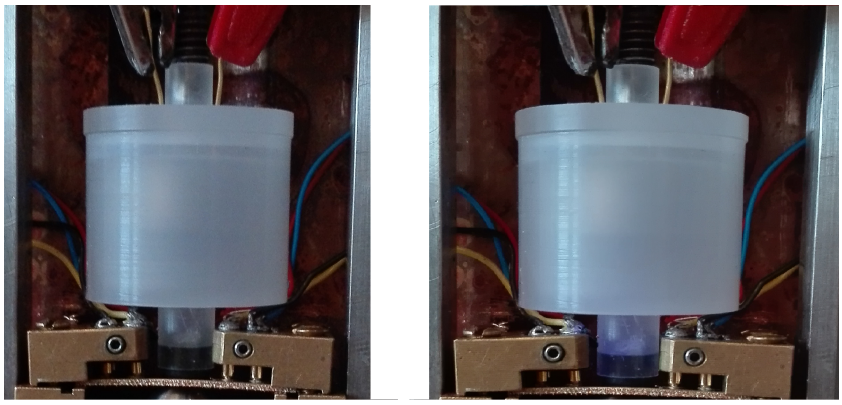

Figure 3.6: The liquid cell with the LED inside. The LED has a wavelength of 365 nm. On the left the LED is turned off and on the right the LED is turned on. As can be seen, the light of the LED does reach the junction.

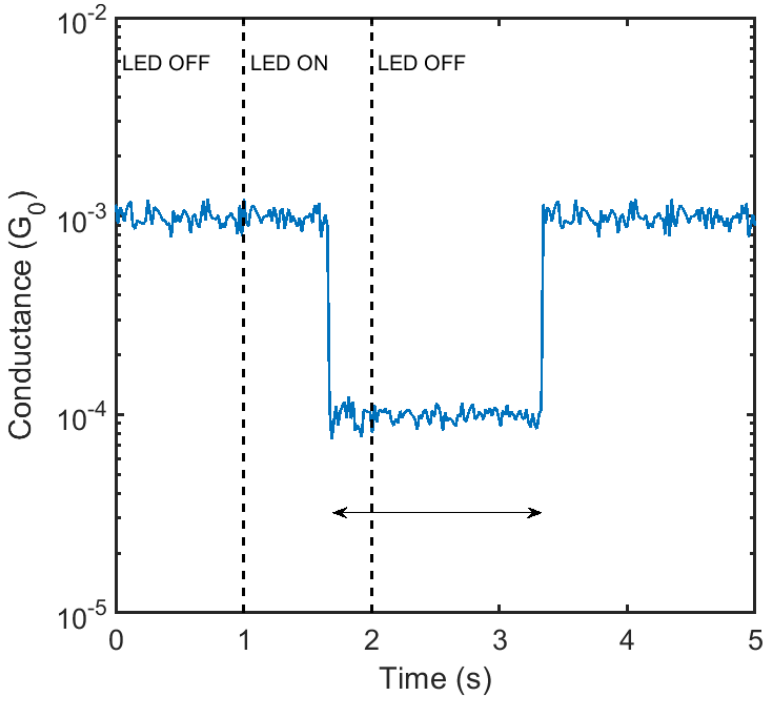

Figure 3.7: A possible realisation of an alternative photoswitch measurement. The LED is turned on between the dashed lines. The arrow indicates the lifetime of the off-state of the molecule.

4

Review Photoswitches

This chapter contains an overview of previous work found in the literature done on photoswitches. The first section will give a conceptual introduction to molecular photoswitches. Subsequent sections will cover a main class of single molecule photoswitches. The last section highlights other successful experiments in the field of molecular photoswitches.

4.1. Photoswitches

Since the beginning, molecular electronics has had the interest of many researchers as it provides the potential of constructing and implementing integrated and multifunctional electrical devices. To accomplish this goal it is essential to investigate the charge transport processes in molecular junctions, since molecules in junctions may display different behaviour than in their bulk form.

The coupling of a molecule with the leads can alter the behaviour of a molecule. A switchable molecule can become a switchable junction. But it is also possible that the coupling of the molecule with the leads results in a passive junction. In that case the molecule loses its functionability. It is also possible to create a switchable junction from a passive molecule. The influence of the coupling on the switchablitity of the molecule can be seen in figure 4.1.

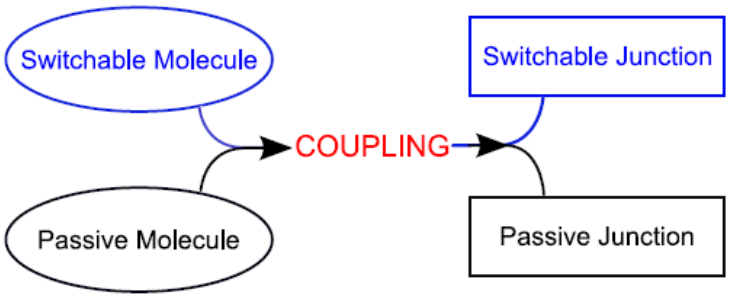

Figure 4.1: A schematic picture of how coupling can influence the properties of a molecular junction. A switchable molecule may keep its switching properties, but it can also loose them. Remarkably, a passive molecule can become switchable in a junction. Taken from [50].

In some switchable junctions, the conductance of the molecule can change under the influence of external stimuli. These stimuli can be electric fields, mechanical stretching, magnetic fields, light irradiation or a change in the pH of the environment. The possibility to change the conductive properties by external stimuli makes these molecules possible building blocks of a new type of miniature switches.

An interesting category of molecules are the photochromic molecules, also known as photoswitches. The energy diagram of a typical photoswitch is shown in figure 4.2. The horizontal axis shows the switching coordinate. This is usually an angle between rings or the distance between atoms inside a molecule. The ground state has two minima, which correspond to the two states of the switch. Switching of the molecule can be achieved upon excitation of the molecule. The relaxation of the excited state can lead to a probabilistic

change of state. The states are separated by an energy barrier of ΔE. Switching between states can also occur if the molecule thermally overcomes the barrier. If the barrier $\Delta E < k_B T$, the molecule can switch thermally and is considered a T-type. When the molecule can not switch thermally because $\Delta E > k_B T$, the switch is a P-type.

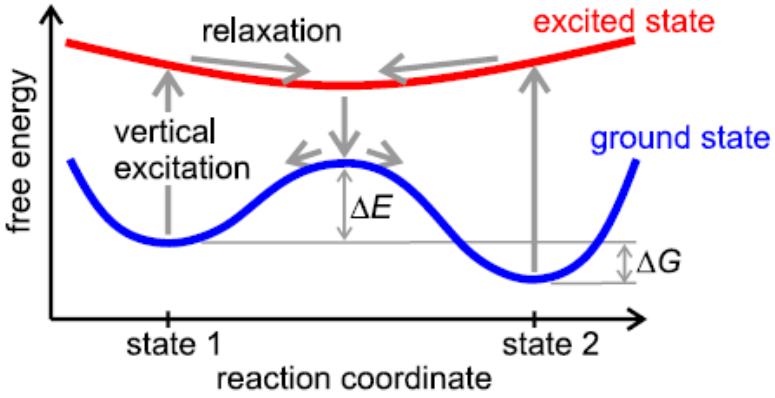

Figure 4.2: An energy diagram of a typical photoswitch. The ground state has a stable state (state 2) and a metastable state (state 1). These states are separated from each other with a barrier of ΔE and the relaxation is driven by ΔG. Exctitation from the ground state to the excited state can trigger the switching between ground states. Taken from [50].

The photoswitches in this overview will be ordered in three categories: the diarylethenes, the azobenzenes and others. These catagories can be justified as follows: the diarylethenes are a well researched group of molecules. A lot of papers have been published about various experiments on diarylethene conductance measurement. The azobenzenes are of interest because they are available at the TU Delft for measurements. That leaves us with the last category: other molecules. This last category will give a quick overview of the results with other forms of photoswitches.

4.2. Diarylethene

The first group of photoswitches are the so-called diarylethene derivatives. These molecules are a promising candidate for electronics because they have a high thermodynamic stability in both states. This molecule is known to reversibly switch in solution, but when they were put in a single-molecule junction, the molecules did not switch both ways or not at all. This chapter will discuss the switching of diarylethene derivates and give an overview of the conductance experiments using diarylethenes as a photoswitch.

4.2.1. Switching mechanism

The switching of these molecules is a photochemical 6-π electrocyclic reaction. These molecules have a high stability because the thermal reaction is hindered by steric effects. The photochemical reaction causes the ring in the middle of the molecule to open or close. Note, that in the closed form there is a π-conjugated path inside the molecule, while in the open form the pathway from one side of the molecule to the other is cross-conjugated. The effect of the switching on the length of the molecule is negligible. Figure 4.3 shows the photoisomerization of the diarylethene molecule. The R in figure 4.3 stands for the rest of the molecule. The switching takes place in the ring of the diarylethene, but the molecule itself can be larger.

The switching mechanism is temperature dependent [12]. Below a temperature of around 120 Kelvin the ring doesn't open anymore. The closing of the ring is not temperature dependent. This means that there is a barrier between the excited state of the closed molecule and the ground state of the open form. To overcome this barrier the electron needs a thermal push over the barrier of approximately 100 meV [12]. To switch from the open state to the closed state, the electron doesn't need a push. So below 120 K the molecule can only switch from open to closed. Above that temperature the molecule can switch both ways. A sketch of the energy levels in the ring-opening process can be seen in figure 4.4. In this sketch the C and O respresent the ground state of the closed and open form respectively and C* respresents the excited state of the closed form. The bump at the right side of the excited closed state respresents the energy barrier of around 100 meV. If the temperature is above 120 K the electron can overcome this barrier and transition to the ground state of the open form, else it relaxes back to the ground state of the closed from.

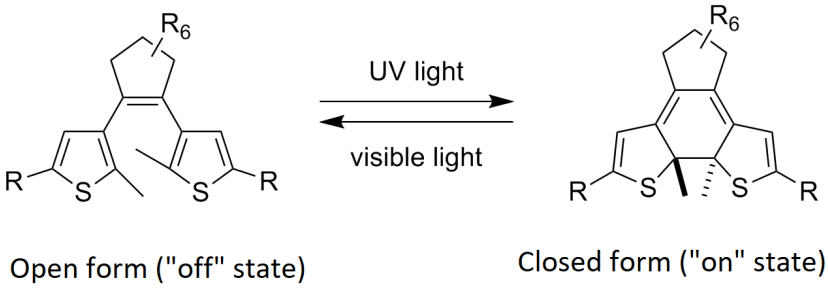

Figure 4.3: The photoisomerization of diarylethene. Upon radiation with UV light the open form transforms to the π-conjugated closed form. The closed form can revert back to the unconjugated open form upon stimulation with visible light. Adapted from [52].

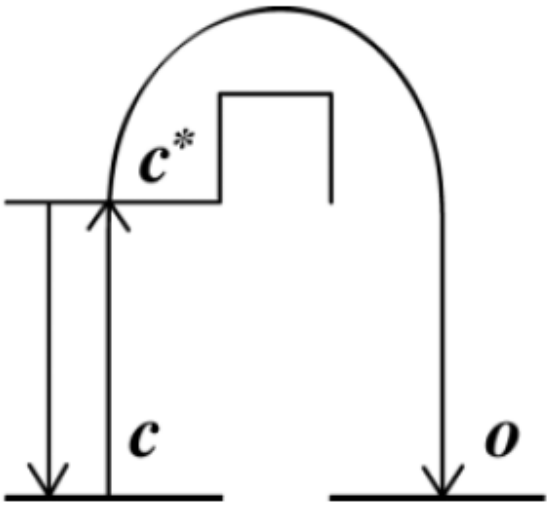

Figure 4.4: A sketch of the energy levels in the ring-opening process. C and O represent the closed and open ground state respectively and C* the excited closed state. An electron in the excited state of the closed form needs to overcome an energy barrier to transition to the ground state of the open form. Adapted from [12].

4.2.2. Origin of difference in conductance between states

The origin of the difference in conductance states has been researched. The open and closed diarylethenes were measured with an STM-BJ [23]. The molecules were switched in solution prior to the conductance measurements. The measurements showed that there is a difference in both the HOMO-LUMO gap and the coupling with the electrodes between the open and the closed state. From the data it became clear that the difference in conductance between the states comes from the difference in coupling with the electrodes.

But the change in coupling does not completely account for the change in conductance. The LUMO and the LUMO+1 lie close together. The two orbitals interfere with each other and reduce the conductance through the LUMO. A way to model this interference was proposed recently [35]. Figure 4.5a shows a schematic representation of this model. The LUMO and the LUMO+1 are very close to each other for the open form. These orbitals interact and the behavior of these two interacting levels resembles the antisymmetric hydrogen bonding. The two levels at different energies can be modelled as two levels at the same energy with a hopping parameter between them. This hopping parameter decreases the transmission probability and further explains the difference in conductance between the two states. For the open state equation 2.3 doesn't hold anymore as the transmission probability has to be replaced by:

$$T(E) = \frac{4\Gamma^2 {t_H}^2}{\left[(E-E_0+t_H)^2+\Gamma^2\right]\left[(E-E_0-t_H)^2+\Gamma^2\right]}. \tag{4.1}$$

An example of $T(E)$ in this cased is shown in figure 4.5b. The transmission probability is reduced because of the "hopping" between the two LUMO levels.

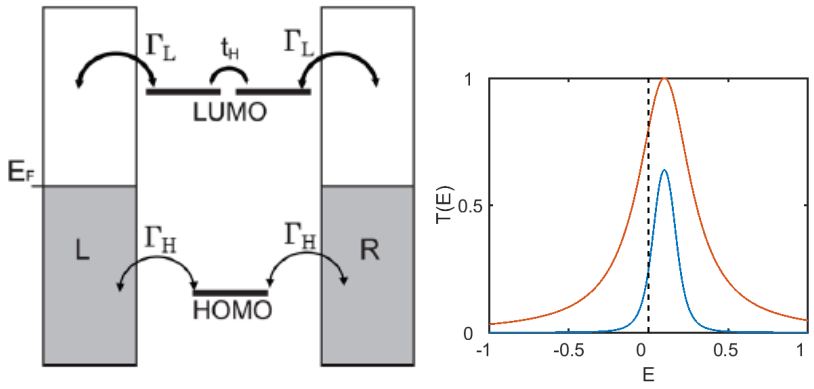

(a) A schematic of the levels in the extended single-level model. The two states of the LUMO are coupled with a hopping parameter t_H to model the interaction between the LUMO and the LUMO+1. Adapted from [35].

(b) A transmission probability plot of the extended single level model together with a plot of the transmission probability of the single level model. The orange curve is without the hopping and the blue curve includes the hopping. Note that both maxima are at the same energy and the amplitude of the whole blue curve is reduced. For both plots $E_0 = 0.1$ V and $\Gamma = 0.1$ eV and for the blue curve $t_H = 0.05$ eV.

Figure 4.5: A schematic of the open state in the extended single-level model. The two states of the LUMO are coupled with a hopping parameter t_H. Figure 4.5a shows the two levels of the LUMO with the hopping between them and figure 4.5b shows the influence of this hopping on the transmission probability of the LUMO.

4.2.3. Single-molecule devices

In the early experiment by Dulic et al., only one-way switching was observed [11]. It turns out that when diarylethene is connected to gold electrodes, the excited state of the open form is quenched by the electrodes, i.e., the excited electron leaks away to the leads before going back to the ground state and is replaced by an electron from one of the leads. As the transition from excited to ground state triggers the opening and closing of the ring, no switching is observed in this process. This can be seen in figure 4.6. This figure shows the energy levels as a function of the switching coordinate. The switching of the molecule takes place along the dashed arrows.

In order to reduce this quenching, linker groups are added to the molecule. These groups reduce the electric coupling between the conjugated parts of the diarylethene and the electrodes. This process is a trade off between switching and conductivity, because when the coupling is reduced, the chance of reversible switching increases, but the conductivity of both states drops. A frequently used method to reduce coupling with the electrodes is to use spacer thiols. These linker groups are not conjungated and increase the distance between the conjugated part of the molecule and the electrode. This increase in distance reduces the coupling. A recent experiment suggests ruthenium as spacer because it decouples the electrode from the molecule, but maintains the conjugated path inside the molecule [32].

Another approach to circumvent quenching, is the use of other electrode materials. There have been experiments with graphene and SWNT electrodes. The SWNT experiments also had one way switching, but in these experiments the diarylethene switched only from open to closed [51]. Recent graphene experiments report a working reversible diarylethene photoswitch[18].

An overview of the single-molecule measurements is given in table 4.1.

4.2.4. Multi-molecule devices

So far, all measurements discussed were done with single molecules, or at least intended for them. There have also been experiments with devices consisting of many molecules. The low yield in photoinduced switching when using gold electrodes is not as big a problem in multi-molecule devices as it is in single-molecule devices, because of the large number of molecules. These multi-molecule devices can be ordered in three categories: self assembled monolayers (SAMs), gold networks and organic transistors. This section will first discuss the devices and conclude with an overview of the experimental results.

A working bidirectional switch was made as a proof of concept [24], consisting of an SAM of diarylethenes between two gold plates. A schematic of this switch can be seen in figure 4.7a. Previous attempts to make

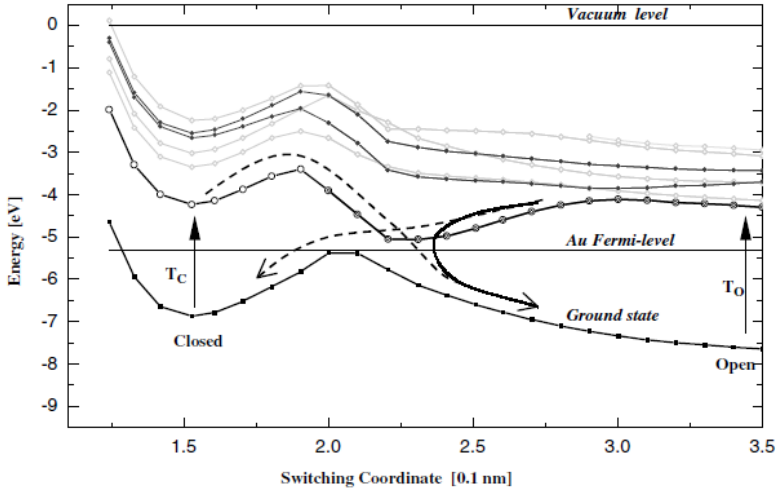

Figure 4.6: Potential energy curves of a diarylethene switch in a gold MCBJ along the switching coordinate q. The switching of diarylethene takes place along the dashed lines. When the open form is excited, the switching is initiated. But when $0.22 < q < 0.25$ nm, the interaction with the gold makes the excited molecule relax back to the open ground state. This process is indicated with the thick, black arrow. Taken from [11].

an SAM switch failed, because the top layer of gold penetrated the diarylethene layer and shorted the switch. This switch has an organic buffer layer between the top of the diarylethenes and the top gold electrode. In the dark the closed state is not stable in this set-up. So this device is not a good candidate to be used as the basis for a memory cell. Another experiment made a small cut in a gold wire and let diarylethenes self assemble in the gap. The device showed a progressive loss of reversibility [32].

The second group of multi-molecule devices are nanoparticle networks. In these networks the space between the two bulk gold electrodes is filled with separate gold nanoparticles. The diarylethenes attach themselfs to the particles and make bridges between them. The distribution of the nanoparticles can be random or ordered. A schematic of a random gold network can be seen in figure 4.7b and figure 4.7c shows a ordered 2D network. In both type of devices there are many connections between the two electrodes and each of these connections is made by many molecules. Both the random and the ordered network showed reversible switching [31][49].

The last group of multi-molecule devices are organic transistors. A sketch of an organic transistor can be seen in figure 4.7d. One of these organic layers is a blend with SWNTs and diarylethenes. In this blend the tubes are randomly ordered in the material and they are connected with diarylethenes. The switching of the diarylethenes changes the conductivity between the tubes and the conductivity of the compound. Another layer is a thin film of diarylethenes. This compound proved to be very stable, it could be left in the dark for multiple days and not lose its state [38].

Table 4.2 shows an overview of the experimental results of diarylethene multi-molecule devices.

4.2.5. Summary

Diarylethenes have been the subject of many photoswitching experiments. The advantages of diarylethene are that both states of the moleule are stable and the length of the molecule does not change considerably upon photoisomerization. The switching mechanism is temperature dependent. The molecule can switch from open to closed at all temperatures, but can only switch from closed to open above 120 K. The difference between the conductance of both states is attributed to a difference in coupling with the leads and interactions between the LUMO and LUMO+1 of the off state.

In single-molecule devices with gold electrodes, the excited state of the closed form can easily be quenched. This hinders the switching, because the relaxation of an electron from the closed excited state to the open ground state triggers the ring opening. To reduce the quenching of the excited state, the coupling between the molecule and the leads was reduced in subsequent experiments. Another way to circumvent this coupling is the use of other electrode materials. Also, the yield of the photoinduced switching is the order of 0.1. So far there has been only one report of a high yield reversible single-molecule switch [18]. Typical switching

Material electrodes	Type of device	High conductance (G_0)	Low conductance (G_0)	Switching ratio	Switching	Ref.
Gold	MCBJ	$1.3 \cdot 10^{-2}$	$1.3 \cdot 10^{-5}$	1000	2	[11]
Gold	STM	$3.2 \cdot 10^{-3}$	$2.5 \cdot 10^{-5}$	130	Y	[14]
Gold	STM				Y	[20]
SWNT	SMJ	$1.5 \cdot 10^{-2}$	$1.9 \cdot 10^{-3}$	7.9	1	[51]
Gold	BJ	10^{-5}	10^{-6}	30	N	[42]
Silicon	AFM	$5.2 \cdot 10^{-5}$	$3.9 \cdot 10^{-5}$	3.4	Y	[46]
Gold	MCBJ				N	[4]
Gold	MCBJ	$4.6 \cdot 10^{-6}$	$1 \cdot 10^{-7}$	38.8	N	[23]
Gold	MCBJ	$7.5 \cdot 10^{-7}$	$2 \cdot 10^{-8}$	10.4	N	[23]
Gold	MCBJ	$1.3 \cdot 10^{-6}$	$1.1 \cdot 10^{-7}$	11.8	N	[23]
Gold	MCBJ	$8.3 \cdot 10^{-7}$	$1.4 \cdot 10^{-7}$	5.9	N	[23]
Graphene	SMJ	$6.9 \cdot 10^{-4}$	$7.5 \cdot 10^{-6}$	107	Y	[18]
Gold	STM	$2 \cdot 10^{-4}$	$5 \cdot 10^{-6}$	40	N	[35]
Graphene	SMJ				Y	[53]

Table 4.1: An overview of single-molecule experiments with diarylethene derivates. Not all experiments included conductivity measurements. The switching ratio is the ratio between the two conductances. Switching is labelled as follows: Y for reversible switching, N for no switching, 1 for switching from the open to closed state and 2 for switching from the closed to the open state. The reversible switching in the experiments with gold electrodes has a low yield.

Type of device	High conductance (G_0)	Low conductance (G_0)	Switching ratio	Ref.
SAM	1.6	0.1	16	[24]
Gold wire	$2.2 \cdot 10^{-1}$	$6.5 \cdot 10^{-2}$	3.4	[32]
Random network	$9.7 \cdot 10^{-4}$	$8.1 \cdot 10^{-4}$	1.2	[17]
Random network	$6.5 \cdot 10^{-4}$	$1.6 \cdot 10^{-4}$	4	[31]
Random network	$6.2 \cdot 10^{-7}$	$6.0 \cdot 10^{-7}$	1.03	[45]
Ordered network	$4.1 \cdot 10^{-5}$	$2.8 \cdot 10^{-5}$	1.5	[49]
SWNT blend	13	4.3	3	[38]
Thin film	$2.6 \cdot 10^{-8}$	$3.9 \cdot 10^{-10}$	67	[13]

Table 4.2: An overview of multi-molecule measurements with diarylethenes. All devices showed reversible switching.

ratios for single-molecule devices are in the order $10^0 - 10^3$.

Multi-molecule devices circumvent the low yield by taking a large amount of molecules per device. There are three main groups of many molecule devices: the SAMs, the nanoparticle networks and the organic transistors. All these devices show reversible switching upon irradiation. The stability and fatige resistance of these devices varies. Typical switching ratios for multi-molecule devices are in the order of $10^0 - 10^2$.

4.3. Azobenzene

The second class of photoswitches are the azobenzenes. These molecules undergo a cis-trans isomerization upon irradiation. The trans form of the azobenzene is shaped like a rod, while the cis form looks like a Γ. The cis form is metastable and relaxes back to the trans state over time or under the influence of light. This isomerization is shown in figure 4.8.

The isomerization of an azobenzene changes the form of the molecule. Therefore the length of the molecule changes too and this change makes it more difficult to make a single molecule switch with azobenzene. The length change is dependent on the excact form of the molecule but in figure 4.8 it is approximately 10 Å [30].

4.3.1. Switching mechanism

In solution azobenze can switch both ways. The switching of azobenzene under irradiation or relaxation happens upon rotation of the double nitrogen bond [9]. This bond has two local minima that correspond to the two isomers. The minimum of the trans isomer is the global minimum and therefore the cis isomer is metastable. The relaxation time of the cis isomer is in the order of hours, but is dependents largely on sidegroups.

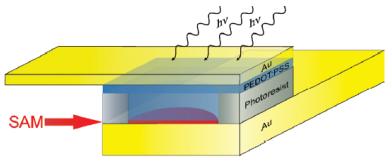

(a) A schematic of the SAM switch. In this experiment 35 devices were created with a diameter varying between $10-100\ \mu m$. Taken from [24].

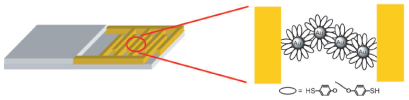

(b) A schematic of a random gold network. The exerpt shows a simplified connection between the two main leads. In reality the connection contains dozens of nanoparticles and the nanoparticles do not form a single line. Taken from [31].

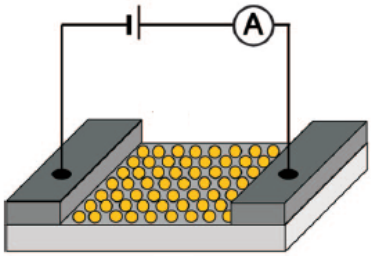

(c) A schematic of an ordered 2D goldparticle network connected by diarylethene molecules. Adapted from [49].

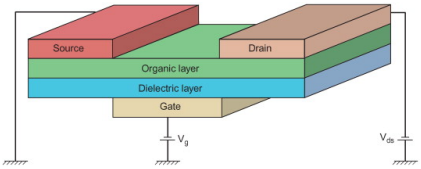

(d) A schematic of an organic thin layer transistor. The diarylethene based compound takes the place of the organic layer. Taken from [36].

Figure 4.7: An overview of multi-molecule devices.

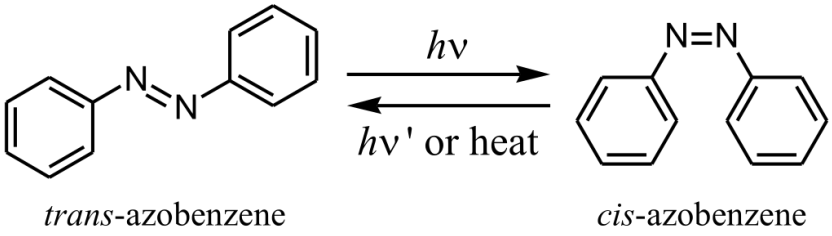

Figure 4.8: The cis-trans photoisomerization of azobenzene. Taken from [41].

4.3.2. Single-molecule devices

The first STM experiments focussed on the effect of the leads on the switching behaviour. It turns out that azobenzene in a junction can be switched by electric fields [1] and by illumination [5][25] while on the substrate. These experiments did not include conductivity measurements.

The isomerization of azobenzene changes the length and orientation of the molecule drastically. This change can break the connection between the molecule and the electrodes, or the isomerization may be prevented by the pull of the electrodes. In MCBJ measurements the switching is suppressed [22]. There are two theories to explain the lack of switching. First there is the coupling between the electrode and the molecule that quenches the excited state. Secondly, the side groups don't have enough flexibility to adapt to the isomerization without breaking the contact to the electrodes. It is possible to do conductance measurements on single azobenzene molecules. But in those measurements, the molecules switch in solution before the measurements start. In the literature there aren't any reports to the best of my knowledge of in-situ switching single-molecule devices using a trapped azobenzene molecule.

A totally different approach to a molecular switch with azobenzene was done very recently [27]. In this experiment the photoisomerization is used to bend a π-conjugated system. A schematic of this mechanism can be seen in figure 4.9. The azobenzene is connected to a π-conjugated system. Upon isomerization, the azobenzene bends the benzene groups and puts stress on the bonds between them. In molecules like this the change in conductance is driven by the change in torsion angles from the isomerization of the azobenzene.

In this molecule the length differs only a few ångström between the two states. This is significantly than in the previously mentioned devices. The angles between the benzene groups have multiple energetic minima. Therefore the system does not necessarily return to the initial state upon reversible switching. This results in a spread of conductances and switching ratios.

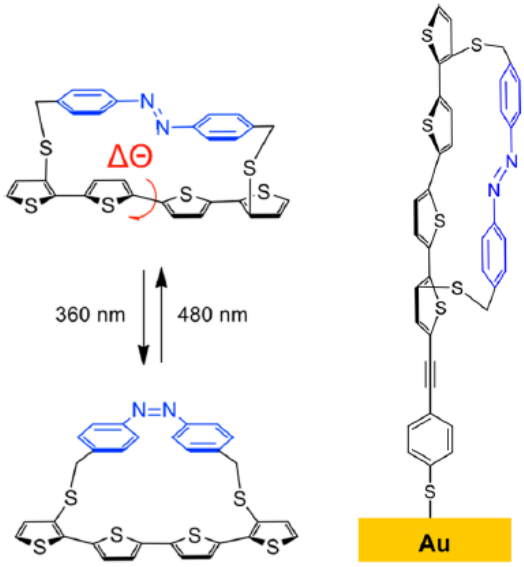

Figure 4.9: The switching mechanism of dynamic π-conjugated systems. Taken from [27].

Table 4.3 gives an overview of single-molecule conductance measurements of using azobenzenes.

Type of device	High conductance (G_0)	Low conductance (G_0)	Switching ratio	Switching	Ref.
MCBJ	$4.9 \cdot 10^{-7}$	$1.6 \cdot 10^{-7}$	2.9	N	[22]
π-switch			$10^0 - 10^3$	Y	[27]

Table 4.3: An overview of single-molecule measurements with azobenzenes.

4.3.3. Multi-molecule devices

The azobenzene multi-molecule devices can be ordered in two groups: SAMs and organic transistors. The SAM devices work differently than the diarylethene ones, because of the length change upon photoisomerisation.

The goal of the first multi-molecule experiments was to create a reversible azobenzene switch [30]. In this experiment a SAM of azobenzenes was measured with an AFM. This device allowed for one way switching; only the trans-cis isomerization was observed. The current presumeably does not go through the azobenzene in this device. The conductance change of the switching corresponds to the conductance change of the difference in tunnel barrier between the tip and the substrate. This device only attaches the azobenzene on one side at the gold substrate. The tip is placed on the sample after switching. Another device consists of an SAM of azobenzenes between graphene [40]. One end of the molecule is chemically bonded to the graphene while the other end is physically bonded. In this set-up the molecules can be switched by light and by voltage pulses. The two graphene sheets have a high flexibility, so this device can be twisted and bended without losing its functionality. Azobenzenes have also been used to make an OFET. This transistor showed reversible switching but had a low switching ratio [26].

Table 4.4 shows an overview of multi-molecule measurements with azobenzenes.

4.3.4. Summary

Azobenzenes switch upon irradiation in solution and are stable in both forms for hours. This stability makes them interesting for research. Unfortunately, the photoisomerization changes the form of the azobenzene

Type of device	High conductance (G_0)	Low conductance (G_0)	Switching ratio	Switching	Ref.
SAM AFM (Pt-Ir tip)	$1.6 \cdot 10^{-5}$	$6.5 \cdot 10^{-7}$	24.6	1	[30]
SAM AFM (Au tip)	$6.5 \cdot 10^{-3}$	$3.2 \cdot 10^{-4}$	20.3	1	[30]
SAM graphene	$5 \cdot 10^{-2}$	$5 \cdot 10^{-3}$	10	Y	[40]
Thin film	$7.9 \cdot 10^{-6}$	$3.6 \cdot 10^{-6}$	1.9	Y	[26]

Table 4.4: An overview of multi-molecule measurements with azobenzenes. Switching is labelled as follows: Y for reversible switching, N for no switching and 1 for switching from the trans- to the cis-state.

drastically. This change in configuration makes it more difficult to create a single-molecule azobenzene photoswitch with reversible switching between leads.

Single-molecule devices with a switching azobenzene in the main conductance path are not found in the literature to the best of my knowledge. The switching breaks the connection with the leads or the switching is suppressed by the leads. To do single-molecule measurements, the molecules switch in solution before getting caught in a junction. A way to circumvent this problem is to make a molecule with azobenzene that does not change its length considerably when it switches [27]. The single-molecule devices have a switching ratio in the order of $10^0 - 10^3$.

Multi-molecule azobenzene devices also have to deal with the length change. In SAMs this length change is used to change the distance between two leads and influence the tunneling current in that way. This leads to a switching ratio in the order 10^1. An azobenzene with long sidegroups is put in an OFET. The change in capacitance of the molecule produces a switching ratio of the order 10^0.

4.4. Other Molecules

In this section other types of photoswitches will be briefly discussed. Only experiments with reversible switching will be discussed.

4.4.1. Spiropyran

A spiropyran (SP) derivate can switch to a merocyanine (MC) both under the influence of light and via a chemical signal. This can be seen in figure 4.10.

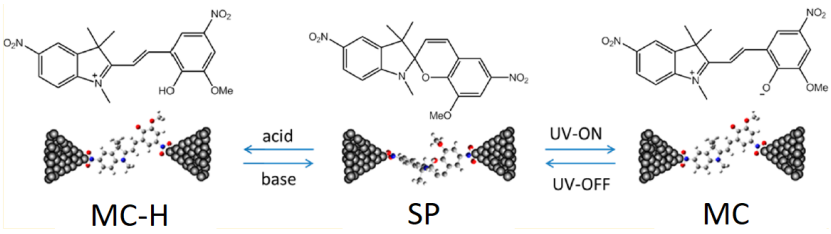

Figure 4.10: Two possible isomerizations of spiropyran derivatives. SP becomes MC upon UV irradiation. But it can also form MC-H if the pH is changed. Both these changes are reversible. The MC and MC-H are conjugated, while the SP form is not. Adapted from [8].

Both ways of isomerization have been measured in an STM-BJ. The non-conjugated form has a conductance of $2.3 \cdot 10^{-2}$ G_0 and both conjugated forms have a conductance of $1.5 \cdot 10^{-1}$ G_0. This results in a switching ratio of 6.5 [8].

4.4.2. Norbornadiene

These molecules are based on the molecule norbornadiene (NB). This molecule can, under the influence of light, transform into its isomer quadricyclane (QC). This process is shown in figure 4.11.

The NB form of this molecule has a conjugated path between the two anchoring groups, while the QC form is not completely conjugated. Furthermore, the tension in the σ-bonds in the QC form forces the current through a longer path. Instead of going through the bond between carbon atom 2 and 3, the current follows the outer ring of carbon atoms 2-1-6-5-4-3. Conductivity measurements were done in a gold STM-BJ. The NB from has a conductivity of $1.2 \cdot 10^{-4}$ G_0 and the QC form has a conductivity of $1.9 \cdot 10^{-5}$ G_0. This photoswitch has a switching ratio of 6.6 [43].

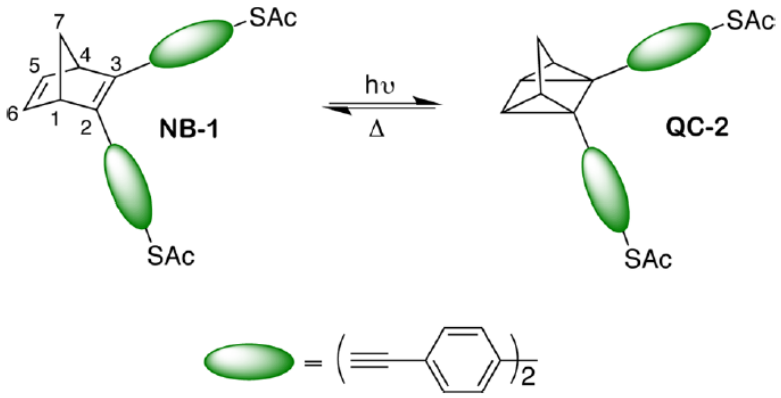

Figure 4.11: The isomerization of the norbornadiene form to quadricyclane form upon irradiation. The inverse process happens under thermal relaxation. Taken from [43].

4.4.3. Dihydroazulene

Dihydroazulene (dha) can switch to vynilheptafulvene (vhf) upon irradiation. This switching opens one of the carbon rings, as can be seen in figure 4.12.

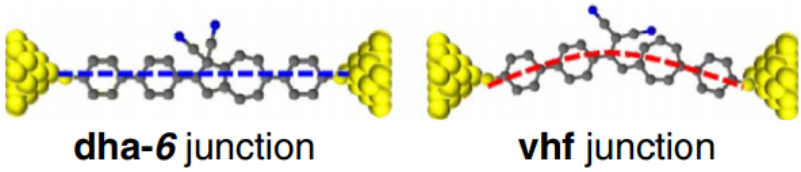

Figure 4.12: The isomerization of the dihydroazule to vinylheptafulvene upon irradiation. Taken from [16].

The states have different interference features that change the conductivity of the molecule inside the junction. Measurements on this photoswitch were done inside an STM-BJ. The conductance of the dha state is in the order of $10^{-3} - 10^{-4.5}$ G_0 and the conductance of vhf is in the order of $10^{-4.5} - 10^{-6}$ G_0 [16]. These wide ranges make it hard to determine a switching ratio.

4.4.4. Dimethyldihydropyrene

Upon irradiation with visible light dimethyldihydropyrene (DHP) switches to cyclophanediene (CPD). It switches back under the influence of UV light or heat. DHP is a polycyclic π-conjugated unit, where CPD is less conjugated as can be seen in figure 4.13.

In an MCBJ the DHP shows a conductance around 10^{-4} G_0 and CPD has a conductance below 10^{-8} G_0. The CPD conductance was below the noise level of the set-up. This results in a switching ratio in the order of 10^4 [37].

4.5. Summary and conclusions

There has been a lot of research on single-molecule photoswitches. These switches could be used as building block for a new type of molecular device. Diarylethenes got a lot of attention because both states are stable for some time and the length of the molecule does not change considerably upon isomerization. The coupling of the diarylethene to leads quenches the excited state of the closed form. To prevent this quenching and allow for reversible switching, the coupling between the molecule and the leads has to be reduced. So far one successful experiment has been reported. Azobenzenes have the disadvantage that the form of the molecule changes drastically when it switches, but the advantage that both form are stable for hours. This change breaks the connection to the leads or the connection to the leads hinders the switching. To circumvent this problem, a large molecule was created that does not change its length much upon switching. Typical switching ratios for single-molecule measurements of both molecules are in the order of $10^0 - 10^3$. Multi-molecule measurements have been done with both molecules. These measurements show limited reversible switching

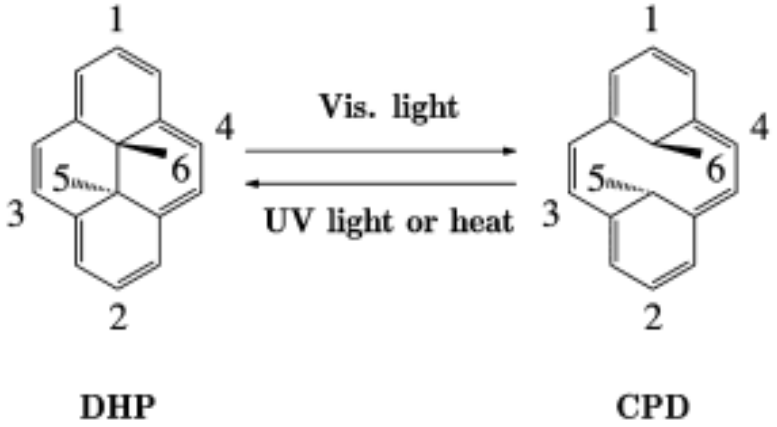

Figure 4.13: The isomerization of the dimethyldihydropyrene (DHP) to cyclophanediene (CPD). The numbers indicate the locations where side- or anchoringgroups can be attached. Adapted from [15].

and usually low conductances or low switching ratios. Four other molecules are shown that show reversible switching in a single-molecule set-up.

The ideal single-molecule photoswitch can be characterized as follows. The molecule must have a clear signature in the 2D histogram in both states. The switching ratio should be at least a few orders of magnitude, so there is a considerable difference in conductance that originates from the switching and not from a difference in configuration. Both the high and low conductance have to be between 10^{-2} G_0 and 10^{-6} G_0 to make sure the conductance can be measured. The switching yield should also be 1 or close to it, to make the switch as efficient as possible. And the molecule should be able to reversibly switch between both states when it is connected to the electrodes. If both states are stable between the electrodes for a long time and the switching yield is 1, it can be possible to make a single-photon switch and use it as memory in new electronics.

5

Measurements of Porphyrin

This chapter contains the first measurements done during the thesis work. In these measurements the conductance of two porphyrins is measured. Porphyrins are a group of molecules with a large conjugated ring as the basis, called porphine. Porphyrins are of interest because of their conjugated backbone, their strong absorption of visible light and low attenuation factor [39]. Figure 5.1 shows the porphine ring, P-1 and P-2. Both porphyrins are almost fully conjugated and have a phenyl ring with two tert-butyl groups on the top and bottom. These bulky butyl groups should prevent the molecule from connecting with the electrodes via these phenyl rings.

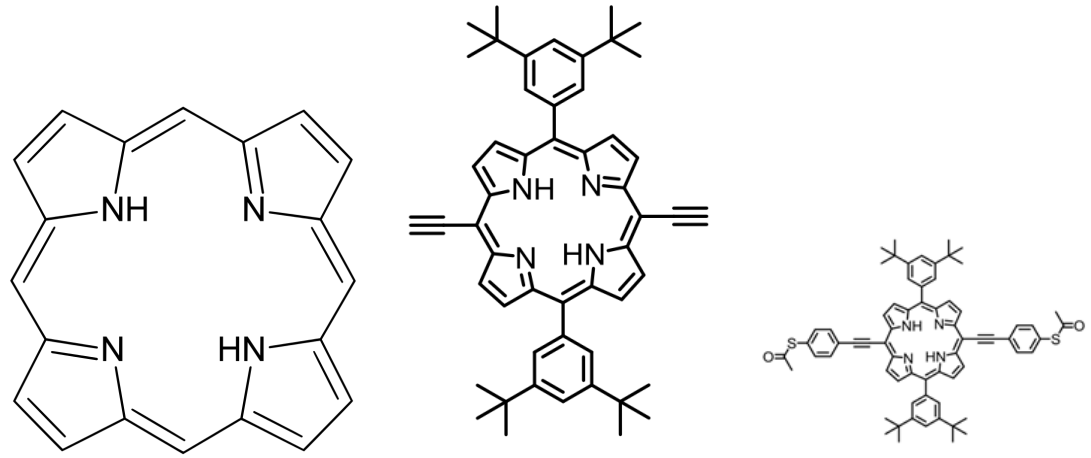

(a) Porphine. (b) P-1. (c) P-2.

Figure 5.1: The core of every porphyrin is the conjugated porphine. The measured porphyrins are P-1 and P-2.

5.1. P-1

P-1 is put in a 0.1 mM DCM solution that is dropcasted upon the sample. The result of the measurements with a bias of 100 mV and a breaking speed of 100 V/s can be seen in figure 5.2a. The 2D histogram does not show conductance plateaus. The 2D histogram does show two areas with increased counts. The first region falls between 1 G_0 and $5 \cdot 10^{-3}$ G_0 from 0 to 1 nm. The second one is between 10^{-4} G_0 and the noise level from 0.2 to 1.5 nm. Figure 5.2 also shows two 2D histograms of other measurements of P-1. Figure 5.2b shows a measurement on the same batch of molecules done in Chili and figure 5.2c show measurements of a batch op P-1 synthesyzed by Jon Hill that was measered in Delft. The Chile measurements also do not show a conductance plateau. The Jon Hill measurements do show a short, 0.6 nm, plateau at $2 \cdot 10^{-5}$ G_0. The Jon Hill measurement looks the most like a molecular signature for P-1. However, this signature could only be replicated once.

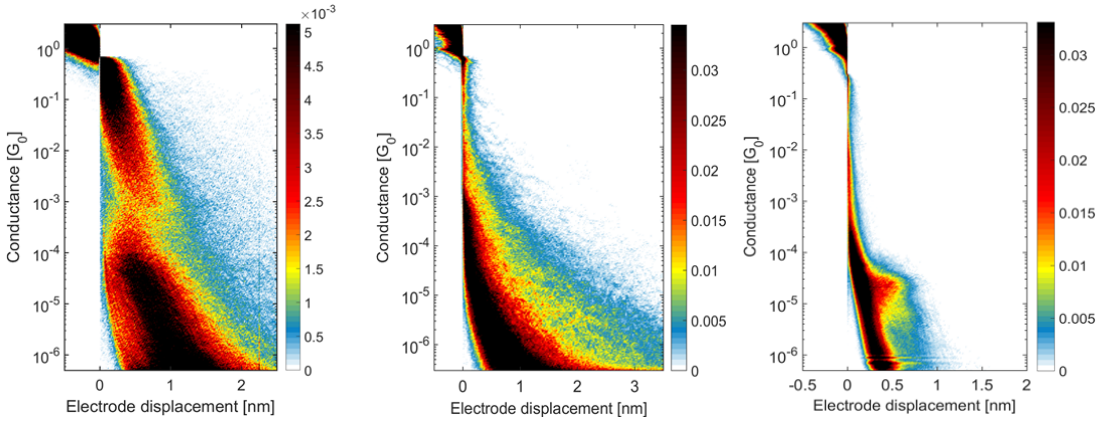

(a) Delft measurement (b) Chili measurement (c) Jon Hill measurement

Figure 5.2: The 2D histograms of several P-1 measurements. All three measurement show different results.

When one looks at individual traces in figure 5.3, there are two different behaviours visible. In figure 5.3a the traces show plateaus at various conductance values. Figure 5.3b shows a staircase like behaviour in the traces. Some of the plateaus are at the same conductance as the plateau found in Japan, but there are also plateaus at other values present. The staircase-like traces seem to display a drop in conductance of a factor 10 every step, but the conductances of the steps differ per trace and the drop also varies every trace. All these factors make it is unclear if the signal originates from single-molecule junctions. The measurements were repeated with different bias voltages and breaking speeds which produced very similar 2D histograms. All runs had both plateaus at different conductances and staircase-like traces. The measurements in Chile also showed staircase-like traces and traces with plateaus at various conductances.

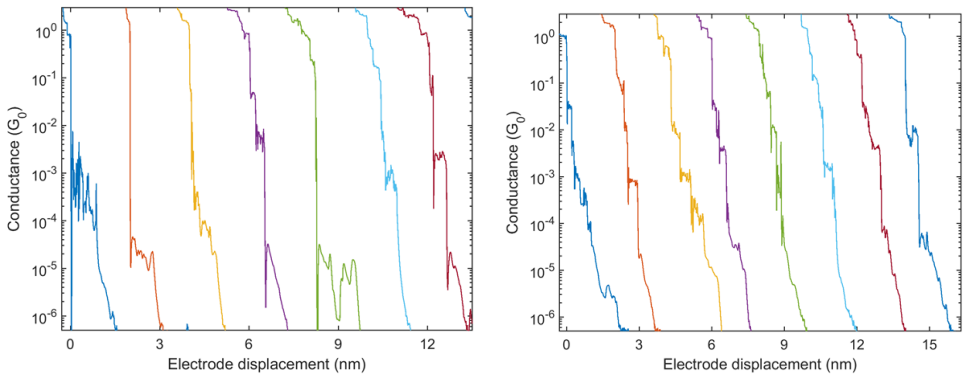

(a) Plateaus at various conductances. (b) Staircase-like traces.

Figure 5.3: Example traces of P-1. There are two different type of traces: plateaus and staircases.

5.2. P-2

P-2 was put in a 0.1 mM DCM solution that was dropcasted on the sample. Figure 5.4 show the results of the first P-2 measurements with a bias of 100 mV and a breaking speed of 200 V/s. The 2D histogram shows counts between 10^{-4} G_0 and 10^{-5} G_0 from 0 to 2 nm. To isolate the molecular traces from the tunneling traces the window filter is used. This window filter produces the 1D histograms visible in figure 5.4b. The window filter shows that the yield of this experiment is around 10%. The 1D histogram shows peaks at $6 \cdot 10^{-6}$ G_0 and $3 \cdot 10^{-5}$ G_0. Most molecular traces have a length around 1 nm, only a few traces reach a length of 2 nm.

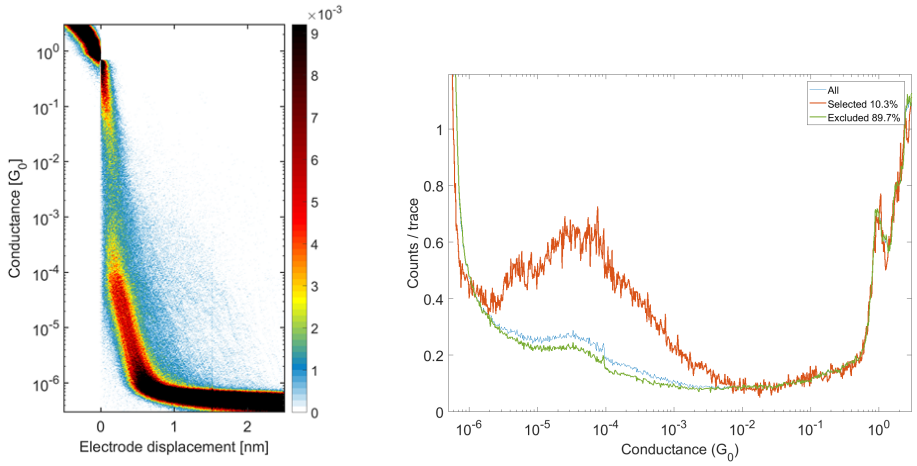

(a) 2D histogram of the P-2 measurement.

(b) 1D histogram after applying window filter.

Figure 5.4: Results of the P-2 measurements. The measurement was done with a bias of 100 mV and a breaking speed of 200 V/s. Figure (a) shows the 2D histogram of the measurement. Figure (b) shows the 1D histograms after applying the window filter to separate the molecular traces from the tunneling traces. The selected traces show peaks at $6 \cdot 10^{-6}$ G_0 and $3 \cdot 10^{-5}$ G_0.

5.3. P-2 with deprotective agent

In following measurements a deprotective agent was added to the solution. This deprotecive agent, tetrabutyl ammonium hydroxide, helps the hydrolysis of the acetyl-protected thiol groups [47]. This favors the connection of the sulfur atomin the anchoring groups to the gold leads. The adding of the deprotective agent should make the molecular signature more pronounced.

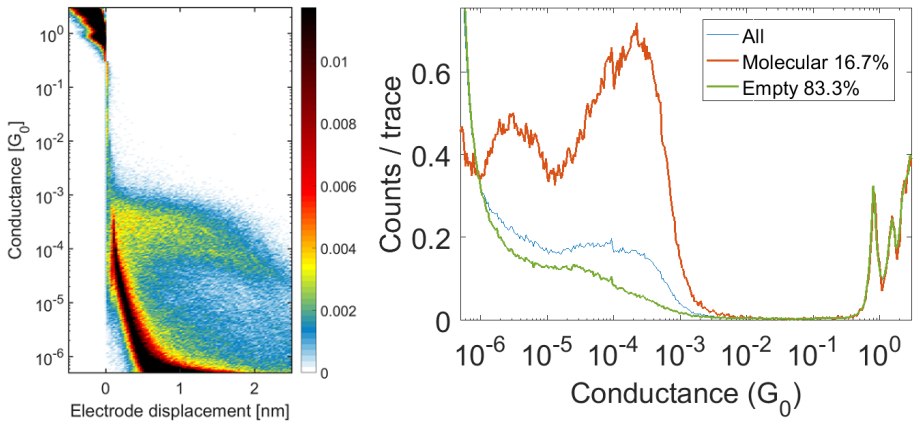

(a) 2D histogram of deprotected P-2.

(b) 1D histogram of deprotected P-2 after applying slope filter.

Figure 5.5: Results of the measurement of deprotected P-2. The measurement was done with a bias of 100 mV and a breaking speed of 200 V/s. Figure (a) shows the 2D histogram of the measurement. Figure (b) shows the 1D histograms after applying the slope filter to separate the molecular traces from the tunneling traces. The selected traces show peaks at $6 \cdot 10^{-6}$ G_0 and $2 \cdot 10^{-4}$ G_0.

The results of the measurement with the TBAH added to the solution can be seen in figure 5.5. This 2D histogram shows a clear molecular signature. A plateau is now easily identified before filtering. Filtering the data with the slope filter shows that the yield of the junction has increased to 17%. Other measurements of deprotected P-2 showed a yield around 30%. Gaussians were fitted to the filtered 1D histogram and revealed conductance values of $6 \cdot 10^{-6}$ G_0 and $2 \cdot 10^{-4}$ G_0.

To check if the TBAH is not the molecule that causes the plateau seen in figure 5.5, a control experiment was carried out. In this experiment a sample was measured with only mixture of DCM with TBAH dropcasted onto the junction. The result of this measurement can be seen in figure 5.6. Both 2D histograms show tun-

neling behaviour. The plateau is not visible after dropcasting the TBAH on the junction, so the TBAH does not produce the molecular signature seen in figure 5.5.

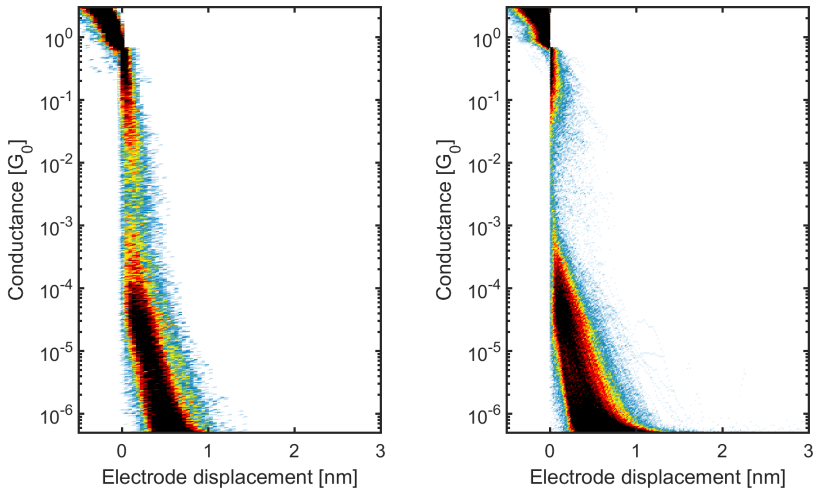

(a) The 2D histogram of the control experiment before dropcasting the solution.

(b) The 2D histogram of the control experiment after dropcasting the solution.

Figure 5.6: The results of the control experiment to see if the deprotective agent, TBAH, produced the molecular signature found in previous measurements. The TBAH does not show up in the histogram after dropcasting.

5.4. Conductance as a function of displacement

The plateau in the deprotected P-2 2D histogram has a downward slope. That means the most probable conductance value changes with the displacement. To gain insight in this relation, the most probable conductance value was determined for each displacement. This can be done by analysing only a slice of the 2D histogram. A vertical slice of the 2D histogram can be summed up over the displacement to form the 1D histogram of a small displacement window. The choice for the width of a slice is the result of conflicting needs. A bigger slice means there are more datapoints to do statistics in each slice, but that also means a loss in displacement resolution. The slices are chosen to be around 0.25 nm wide. This width is of the same order of magnitude as the width that is used in other papers in this procedure [21]. The most probable conductance value for each displacement can be found by fitting Gaussians to the corresponding 1D histogram.

Figure 5.7 shows this process. Figure 5.7a shows a comparison of the 1D histograms obtained from each of the eight slices. The peak of the histograms show two trends. They move to a lower conductance value and their amplitude decreases. Two Gaussians are fitted to each 1D histogram to separate the counts from the molecular and tunneling traces. The peak of the fit of the molecular traces is added to the 2D histogram in figure 5.7b. The black dots follow the plateau accurately.

The same analysis can also be carried out on other measurements of molecules. Figure 3.3d shows a molecular 2D histogram with two horizontal plateaus. The molecule in this measurement is OPE-3. These measurements, along with other OPE molecule measurements, have been carried out in the van der Zant lab before the start of this thesis. The relation between most probable conductance and displacement of this plot was determined by slicing the 2D histogram up in fourteen pieces from 0.5 to 2 nm. Three Gaussians were fitted to the 1D histograms on a log-normal scale. Two Gaussians are to account for both the plateaus and the third one is to fit the tunneling traces. The result can be seen in figure 5.8. Figure 5.8a shows the 1D histograms of the fourteen slices. The peak around 10^{-3} G_0 decreases in amplitude as the displacement increases. The fits cannot distinguish this peak beyond a displacement of 1.25 nm.

5.4.1. End of plateau conductance value

These previously done OPE-3 measurements showed that the most probable conductance value varies with yield [6]. This conductance value was obtained by fitting the 1D histogram after using the slope filter to select the molecular traces. The conductance value of the fully strechted end-to-end connection of the molecule

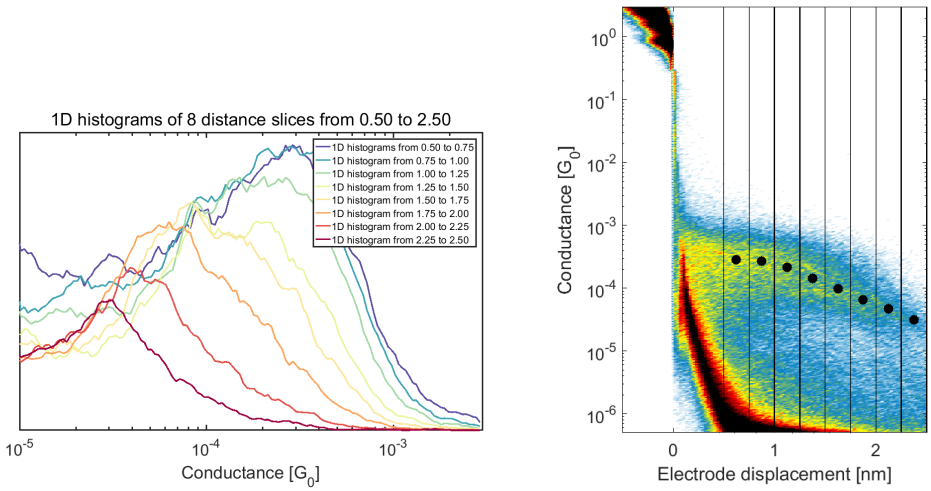

(a) The 1D histograms of all the slices. Two Gaussians were fitted to each histogram.

(b) The 2D histogram of deprotected P-2 with peaks of the fit added as black dots.

Figure 5.7: Finding the relation between the most probable conductance of deprotected P-2 versus displacement.

between two electrodes is most likely the conductance at the end of the plateau. This end-of-plateau conductance value should than be the closest value to the molecular conductance. If this end-of-plateau conductance value is a more accurate conductance value, than this conductance value should vary less between different measurements of the same molecule. The end-of-plateau conductance value can be found with the analysis introduced in the previous section.

In figure 5.9 the end-of-plateau conductance value is compared with the conductance value obtained by fitting the filtered 1D histogram for both OPE-3 and deprotected P-2. Figures 5.9a and 5.9c show both conductance values. The red squares represent the conductance value obtained by fitting the filtered 1D histogram and the blue triangles show the end-of-plateau conductance value. The green triangles in figures 5.9b and 5.9d show the ratio of these two conductance values.

Figures 5.9a and 5.9c both show that the spread in conductances is smaller for the end-of-plateau conductances than the filtered 1D histogram. With both molecules the fit of the filtered 1D histogram produces a higher conductance value than the end-of-plateau conductance value for all yields. The fitted 1D histogram conductance of OPE-3 increases with increasing yield. This trend is not present in the deptrotected P-2 conductances. This behaviour can also be observed in figures 5.9b and 5.9d. The ratio of deprotected P-2 conductances shows no increasing or decreasing trend, but stays relatively stable. The ratio of the OPE-3 conductances also shows the increasing trend with increasing yield. The red line is a linear fit of the ratio of conductances versus the yield. This line is not based on any models or theories, but is added as a guide to the eye. It should be noted that the spread in yield in the deprotected P-2 measurements is not as large as the spread in the OPE-3 measurements. A measurement of deprotected P-2 with a higher concentration did not produce a higher yield measurement.

5.5. Conclusions

The P-1 measurements were not in accordance with the Jon Hill measurements. There are traces with plateaus at various conductance values and staircase like traces present. The measurements show similar features as the Chile measurement. It is unsure if the molecule is measured at all.

The P-2 measurements revealed conductance peaks at $6 \cdot 10^{-6}$ G_0 and $3 \cdot 10^{-5}$ G_0. The yield of this measurement was 10% and most traces did not reach the full length of 2 nm. Adding a deprotective agent to the P-2 solution before dropcasting increased the yield to 30%. The length of the traces also increases when TBAH is added to the solution. With TBAH in the solution the conductance peak shifts from $3 \cdot 10^{-5}$ G_0 to $2 \cdot 10^{-4}$ G_0. To check if the observed molecular signature is of the P-2 and not the TBAH a control experiment was carried out with TBAH in a solution without any P-2. This experiments showed that TBAH does not show up in the measurements itself and the found conductance values belong to deprotected P-2.

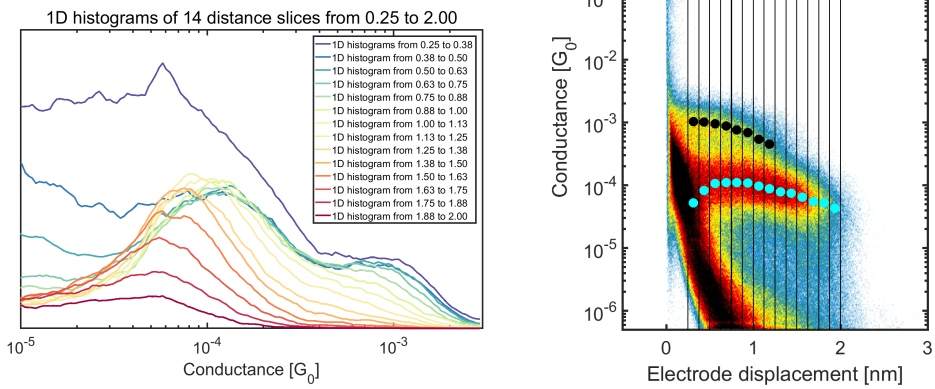

(a) The 1D histograms of the individual slices. Three Gaussians are fitted to each histogram.

(b) The sliced up 2D histogram of OPE-3 with the peaks of the fit added as black and cyan dots.

Figure 5.8: Finding the relation between the most probable conductance of OPE-3 versus displacement. The higher peak can no longer be distinguished after 1.25 nm.

The conductance of deprotected P-2 is dependent on the displacement. By slicing up the 2D histogram, converting them to 1D histograms and fitting them, the relation between conductance and displacement is computed. This analysis is also carried out on OPE-3 measurements done in the van der Zant lab before the start of this thesis. The 2D histogram of OPE-3 shows two plateaus close together which can be separated with this technique.

This slicing technique is also used to determine the end-of-plateau conductance value. This conductance value is most likely the value of the fully streched end-to-end configuration of the molecule. This end-of-plateau conductance value shows less variation between measurements than a fit of the filtered 1D histogram for various yields. Therefore this conductance value is a better estimate of the most probable conductance value of a molecule. The ratio between the conductance value from the filtered 1D histogram and the end-of-plateau conductance value as a function of yield showed different behaviour for deprotected P-2 and OPE-3. The ratio increases as the yield increases for OPE-3, but shows no clear yield dependence in deprotected P-2 measurements.

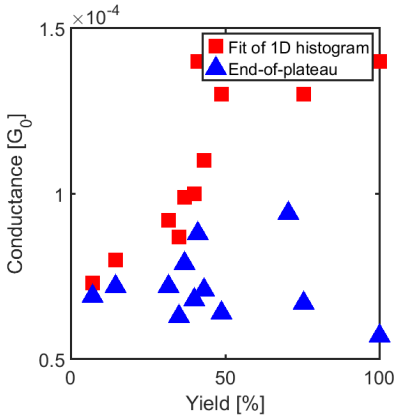

(a) OPE-3 conductance values.

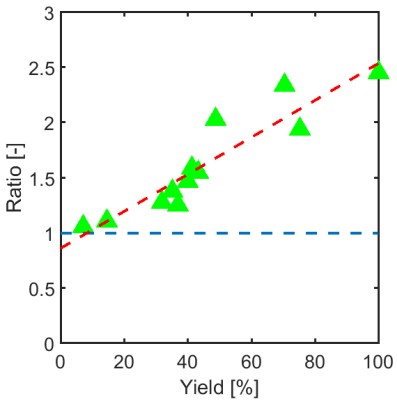

(b) Ratio of OPE-3 conductance values. The red line is added as a guide to the eye.

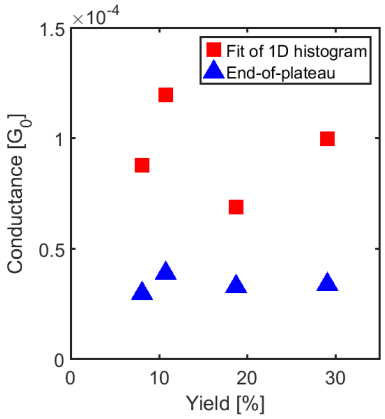

(c) Deprotected P-2 conductance values.

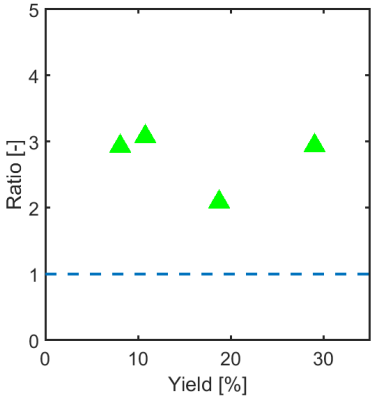

(d) Ratio of deprotected P-2 conductance values

Figure 5.9: The difference between the most probable conductance value obtained from fitting the 1D histogram (red squares) and the end-of-plateau method (blue triangles). The green triangles show the ratio of the two values.

6

Measurements of Spiropyran

This chapter contains the measurements of the photoswitching molecule SP-2. This molecule was measured by Darwish et al. in an STM-BJ and showed reversible photoswitching [8]. This experiment attempts to reproduce the results of Darwish et al. in an MCBJ set-up. For these measurements the available set-up was adapted to allow for an LED to be present inside the liquid cell. The liquid cell is used instead of dropcasting because it is unknown if SP-2 can switch when the molecule is in contact with the gold electrodes.

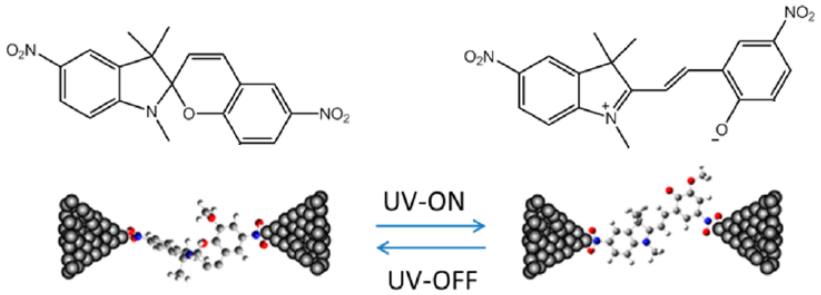

Figure 6.1: The structure of SP-2 (left) and MC-2 (right) together with a 3D redering of how they look inside a junction. Adapted from [8]

SP-2 is a spiropyran and can be seen in figure 6.1. The ring with the oxygen inside opens upon irradiation with UV light to form the merocyanide MC-2. This ring opening creates a conjugated path inside the MC-2 and makes the molecule planar. This conjugated path should result in a higher conductance value. The SP-2 state has a lower free energy and therefore the MC-2 will switch back to SP-2 by thermal relaxation if the LED is turned off. The time it takes to switch back is a few seconds.This means that in order to measure MC-2 the LED has to remain on to keep pumping the SP-2 to MC-2.

All the SP-2 measurements were done inside the new liquid cell with the LED above the junction. The solution in the liquid cell has a concentration of 0.1 mM and the solvent is a 10:1 mesitylene:DCM mixture.

6.1. Note on timescales

Before the measurements can start, relevant timescales have to be considered. These timescales determine if the switching behaviour can be measured at all. Relevant timescales include the switching time of the molecule, the relaxation rate, the time an electron is on the molecule. In our SP-2 measurements the switching is almost instantanious. The relaxation time of SP-2 in solution is about a second. Typical Γ values for MCBJ experiments are in the order of 10^{-3} eV. That means an electron spends approximately 10 ps on the molecule. The time it takes to collect the breaking trace is less than a second. Considering these timescales, it should be possible to measure both states of the molecule in an MCBJ.

It is also important to know the amount of photons involved in the experiment. In our set-up the power of the LED is 100 mW. Combining this with a wavelength of 365 nm means that the LED is producing $1.8 \cdot 10^{17}$ photons per second. In the liquid cell there is usually around 0.2 mL of 0.1 mM solution present. That mounts up to $1.2 \cdot 10^{16}$ molecules in the solution. This results in every molecule getting hit with around ten photons per second.

6.2. Measurements in the dark

The first measurement of SP-2 was done without the switching of the LED. The aim of this measurement was to see if the molecule can be measured at all in an MCBJ. The 2D and 1D histogram of this measurement can be seen in figure 6.2.

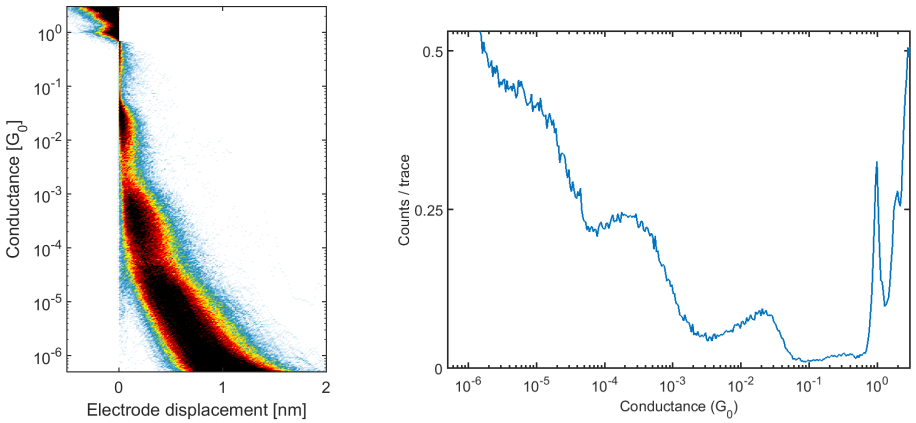

(a) The 2D histogram of the SP-2 measurement.

(b) 1D histogram of the SP-2 measurement.

Figure 6.2: Unfiltered SP-2 measurement without the LED. In this experiment the bias was 200 mV and the breaking speed was 100 V/s. The conductance peaks at $2.5 \cdot 10^{-4}$ G_0 and $1.6 \cdot 10^{-2}$ G_0 in the 1D histogram.

The histograms shows two clear conductance values. The first value is $1.6 \cdot 10^{-2}$ G_0 and the second is $2.5 \cdot 10^{-4}$ G_0. There is also a shoulder of a peak visible around 10^{-5} G_0 in the 1D histogram, but it does not correspond to a visible plateau in the 2D histogram. The first peak is comparable with the values found by Darwish et al. That experiment found conductance values of $1.5 \cdot 10^{-2}$ G_0 and $4.5 \cdot 10^{-2}$ G_0 for this molecule [8]. The peak at $2.5 \cdot 10^{-4}$ G_0 was not reported before. Aspects that may be important when comparing the conductance values in these experiments are the difference in method and electronics. More specifically, the difference between an MCBJ and an STM-BJ and the use of a logarithmic amplifier versus a linear amplifier. The used set-up contains a logarithmic amplifier that allows the measurement of conductances below 10^{-4} G_0. The second peak could be hidden in the noise or below the detection limit if a linear amplifier is used.

The slope filter was unable to filter the traces with short plateaus from the tunneling traces. To further analyse the data, the clustering method was used. The traces were sorted into four classes. The choice of four classes was an initial guess to account for tunneling traces, a class for each peak and a class with both peaks. These settings produces three classes with molecular traces and a class with tunneling traces. One of the molecular classes can be seen in figure 6.4. The two other molecular classes look similar to this class, but with slightly lower amplitudes in the 1D histograms. There is no molecular class with only one of the two peaks present in the histograms. The last class consists of tunneling traces. The tunneling class contains 24.5% of the total traces, so the yield of the measurement is 75.5%. Even though three classes look alike, splitting the data in two classes is not preferable. If the data is splitted in two or three classes, none of the classes contains only tunneling traces.

6.3. Measurements with switching LED

Next the influence of the LED on the conductance was measured. The LED was switched on and off every 500 traces. The peaks around 10^{-2} G_0 and 10^{-4} G_0 could also not be reproduced in these measurements. Variation of concentration, bias voltage and breaking speed did not produce the once found behaviour. Before injecting the solution into the liquid cell the vial was placed in front of the LED to ensure the swichting of the molecule in solution. The results from one of these measurements can be seen in figure 6.5. This figure shows the 1D histogram with the LED on and off with a red and blue line respectively. The conductance values from figure 6.2 are not found even with the LED off. The lines of both histograms overlap almost perfectly, so the influence of the LED is not visible, if there is any effect at all.

For a consistent analysis of the data, these measurements were also analysed with the clustering method.

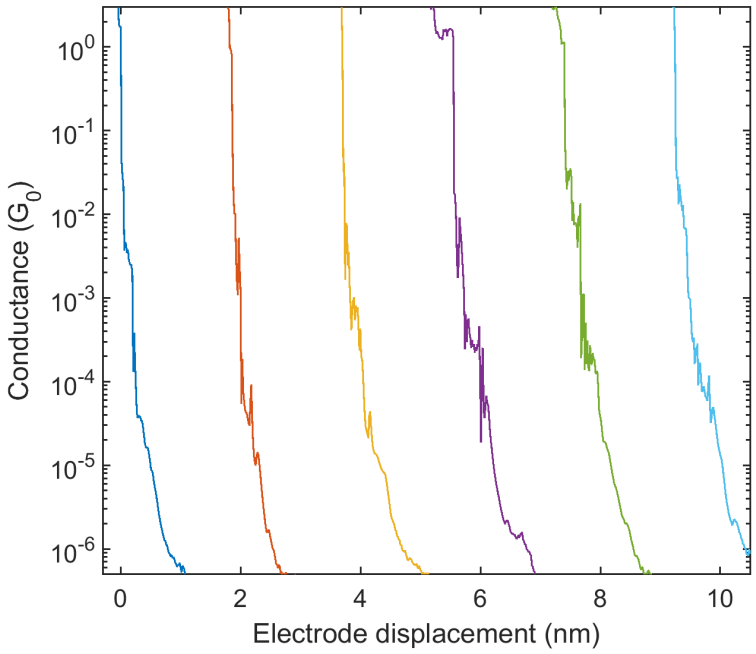

Figure 6.3: Example breaking traces of SP-2. In all the traces there are counts around both conductance values.

The clustering method produced three classes with the LED on and off. Figure 6.6 shows the 1D histograms of the three clusters with the LED off and figure 6.7 shows the 1D histograms of the clusters with the LED on. The 1D histograms of the clusters with the LED off look very similar to those with the LED and represent similar percentages of the traces.

The temperature in the lab went up during the weekend between the measurements without and with the LED. To check if the increased temperature had any effect on the measurements the set-up was cooled down, by surrounding the protective cup of the junction with ice water. This set-up and the measured 1D histograms can be seen in figure 6.8. The molecular signature did not appear after cooling down the set-up.

6.4. Conclusions

This chapter presented the measurements that were done on SP-2 in the illuminated liquid cell in an MCBJ. The SP-2 measurements were done to see if the new liquid cell with the LED works as intended and if the results of Darwish et al. could be replicated in an MCBJ. The first measurements without the LED switching showed conductance values of $1.6 \cdot 10^{-2}$ G_0 and $2.5 \cdot 10^{-4}$ G_0. The first value is comparable to previously found values. The second value has not been found before. These results were not reproducible. Measurements with the LED switching on and off every 500 traces did not show a molecular signature. Variation of the measurement parameters did not reproduce the once found behaviour. The influence of the LED on the conductance of the molecule was not found.

The conductance peaks of $1.6 \cdot 10^{-2}$ G_0 and $2.5 \cdot 10^{-4}$ G_0 were found once in a single measurement. These peaks could be attributed to the SP-2 inside the liquid cell. But it is not certain if those peaks do realy correspond to the molecule, because the results could not be replicated.

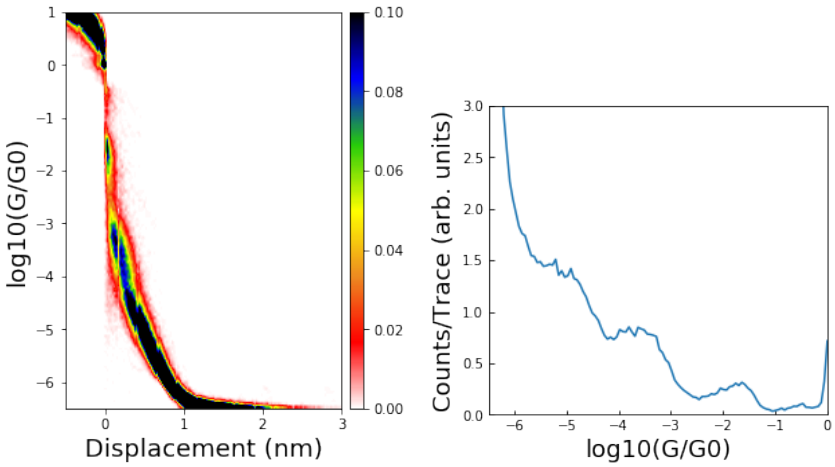

(a) The 2D histogram of class 1.

(b) The 1D histogram of class 1.

Figure 6.4: 1D and 2D histogram of class 1. Class 1 contains 24.5% of the traces. The classes were obtained by letting the clustering method make 4 clusters. Two of the other classes look like class 1, but with lower amplitudes and the last class contains only tunneling traces.

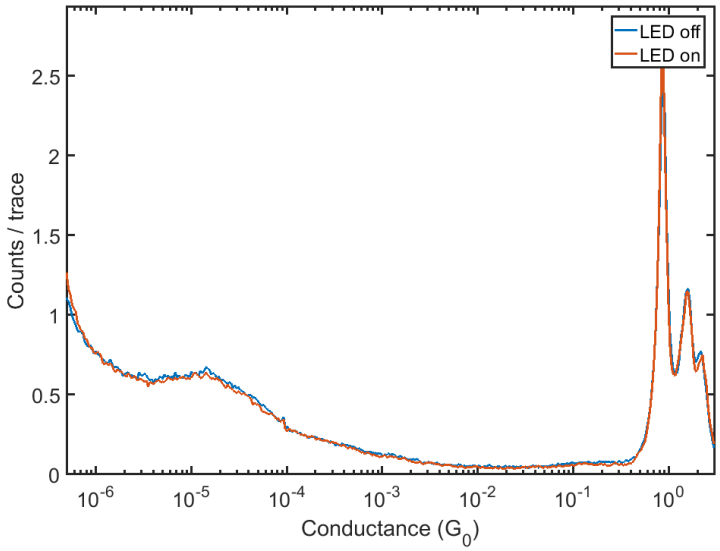

Figure 6.5: 1D histogram of SP-2 measurement with a bias of 100 mV and a breaking speed of 100 V/s. The previous results could not be reproduced. The LED does not seen to have an influence on the measurement.

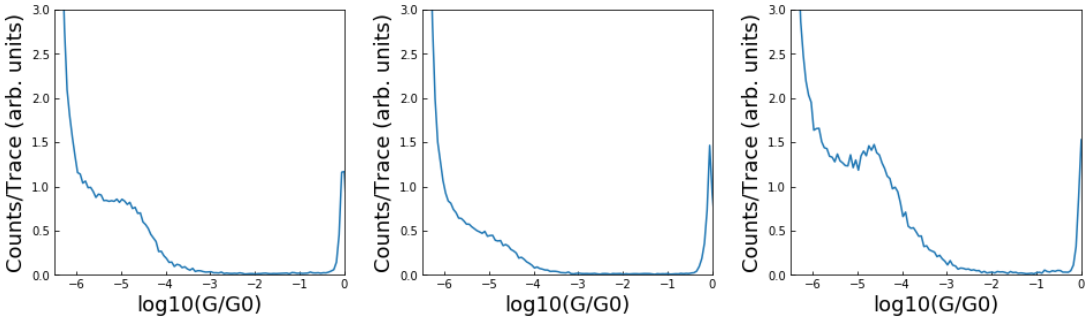

(a) The 1D histogram of class 1. This class has a peak at $7.2 \cdot 10^{-6}$ G_0 and contains 33% of the data.

(b) The 1D histogram of class 2. This class contains the tunneling traces and contains 45% of all traces.

(c) The 1D histogram of class 3. This class contains dirty traces and consists of 22% of the traces

Figure 6.6: The 1D histograms of the three "LED off" clusters of the measurement with the switching LED.

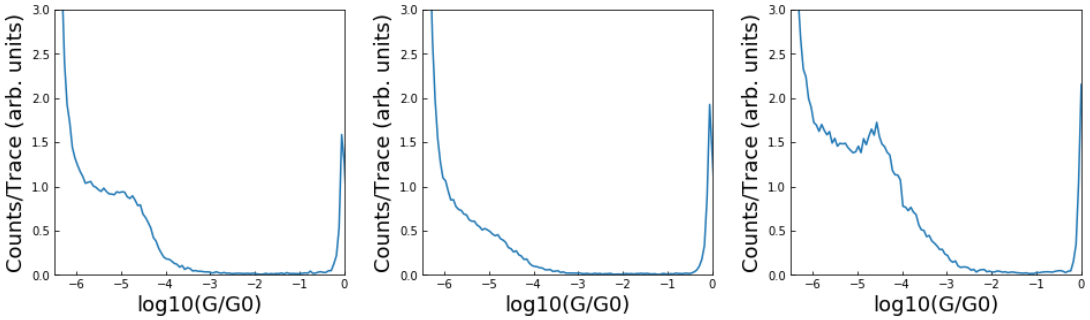

(a) The 1D histogram of class 1. This class has a peak at $7.8 \cdot 10^{-6}$ G_0 and contains 35% of the data.

(b) The 1D histogram of class 2. This class contains the tunneling traces and contains 42% of all traces.

(c) The 1D histogram of class 3. This class contains dirty traces and consists of 23% of the traces

Figure 6.7: The 1D histograms of the three "LED on" clusters of the measurement with the switching LED.

(a) Cooling down the set-up. The bucket is filled with ice water.

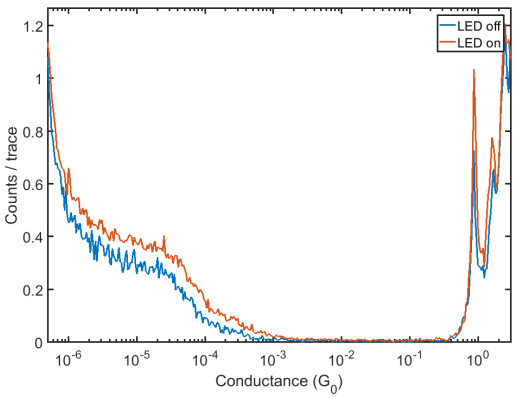

(b) 1D histogram of SP-2 measurement with a bias of 100 mV and a breaking speed of 100 V/s in the ice water.

Figure 6.8: The cooled down set-up and the resulting 1D histogram for the LED off and on. Cooling down the set-up did not make a difference in the result.

7

Summary and Outlook

7.1. Summary

The first part of this thesis consists of a review of the literature on molecular photoswitches with a focus on single-molecule measurements. Most attention was given to diarylethenes and azobenzenes. In the research of diarylethene much effort was put in achieving reversible switching. The switching is quenched from open to closed form because of the coupling between the molecule and the leads. This can be overcome by reducing the coupling or adjusting the leads. So far only working results have been reported on a graphene junction with diarylethene. In case of gold electrodes reversible switching is not archieved yet. In case of azobenzene the difficulty is the large change in length when the molecule switches. This change breaks the connection to the leads or the leads prevent the molecule from switching. This problem was circumvented by designing a larger molecule with a backbone that does not include the azobenzene. The switching of the azobenzene strains the backbone to reduce the conductance. Multi-molecule devices have been measured based on both molecules to show reversible switching. But the switching in these cases is limited.

The second part of the thesis consists of MCBJ conductance measurements on molecules. The available set-up was improved with a liquid cell capable of hosting an LED for measurements of photoswitches in solution. During measurements the solution stays in the cell for over two days and the junctions are stable for over thousands of traces. To use this cell a new measurement protocol was created to distinguish between the influence of the LED and external influences. This illuminated liquid cell makes it possible to research the influence of light on the conductance of molecules in an MCBJ. This makes the new liquid cell a valuable tool in the research of molecular conductances in an MCBJ.

Two of the measured molecules in this work are the porphyrins P-1 and P-2. The measurements of P-1 remained inconclusive. The measurements showed staircase like traces and traces with plateaus at various conductance values. It is not clear if the molecule is measured at all. The P-2 measurements showed conductance peaks at $6 \cdot 10^{-6}$ G_0 and $3 \cdot 10^{-5}$ G_0 with a yield of 10%. Adding the deprotective agent TBAH just before dropcasting has three effects. First the yield increases to 30%. Second, the length of the plateaus increases. And third, the conductance peak at $3 \cdot 10^{-5}$ G_0 disappears and a peak at $2 \cdot 10^{-4}$ G_0 is now visible. A control experiment with TBAH added to a solution without molecules showed that TBAH does not show up in the histograms itself. In the analysis of P-2, the conductance was plotted versus the displacement. This was compared with OPE-3 and showed two different kinds of behaviour. P-2 showed a decrease in conductance while the conductance of OPE-3 did not vary significantly with increasing displacement. This tool was used to investigate the relation between yield and most probable conduction for P-2 and OPE-3. The end-of-plateau conductance value did show less variation than the fit of the 1D histogram with both molecules. These results suggest that the end-of-plateau value is a good candidate for estimating the conductance of the molecule in an end-to-end configuration.

The adapted liquid cell was used to measure the photoswitching molecule SP-2. One measurement revealed the conductance value of $1.6 \cdot 10^{-2}$ G_0 that is similar to a previously reported value and also a new previously unreported conductance of $2.5 \cdot 10^{-4}$ G_0. This result could not be replicated in later measurements. Measurements with the switching LED with various measurement parameters did not reproduce the two conductance peaks. Therefore the influence of the LED on the conductance cannot be determined. It is not certain if the two peaks really originate from the SP-2.

7.2. Outlook

Of the measured porphyrins only the P-2 gave a result. Other porphyrins are already created and are ready to be measured in Delft or Chile. These porphyrins could be a basis for a model system to investigate new properties of molecules in conductive measurements. If a porphyrin has a clear and distinctive molecular signature, an inorganic atom, like iron or zinc, can be added to the center of the porphyrin. These metallic centers can give rise to new features.

In this work only one molecule was measured in the adapted liquid cell. These results of these measurements were not reproducable. It would be interesting do another SP-2 measurement with the molecule dropcasted on the sample. The attention should also be shifted to other molecules. The literature review showed that there are not yet any reports of a reversible single-molecule photoswitch in a gold MCBJ. The diarylethenes look like a promising candidates for reversible switching. If the switching part of the molecule can be decoupled from the leads enough, it could allow for reversible switching. Ways to achieve this decoupling could be spacer thiols or different kind of anchoring groups.

7.3. Acknowledgement

This thesis has my name on it, but I could never have done it alone. During my time in the van der Zant lab I came across several people that have helped me out with all kind of problems. First I want to thank Herre for guiding me during this thesis. During our many talks, formal and informal, you have helped me tremendously. Your ability to step out of the details and see the bigger picture without losing the important concepts is admirable.

Next I would like to thank my daily supervisor Davide. You are truly the rock on which the van der Zant lab church is built. You introduced me to the experimental world of molecular electronics and you really know everything there is to know about the set-ups. You were always available for questions and willing to help me. Under your guidance I learned a lot, you are a great mentor and coworker. When you finish your thesis, the lab will have a hard task replacing you.

I also want to thank all the other people I have had the opportunity to work with in the lab: Ignacio, Pascal, Damien, Sabina, Jacqueline, Joeri, Alfredo, Jochem and Esmee. Working in the lab was always a pleasure for me because of the friendly atmosphere. Thank you all for the discussions and the laughter over the past months.

Bibliography

[1] M. Alemani, M.V. Peters, S. Hecht, K. Rieder, F. Moresco, and L. Grill. Electric field-induced isomerization of azobenzene by stm. Journal of the American Chemical Society, 128:14446–14447, 2006. DOI: 10.1021/ja065449s.

[2] A. Aviram and M.A. Ratner. Molecular rectifiers. Chemical Physics Letters, 29:277–283, 1974. DOI: 10.1016/0009-2614(74)85031-1.

[3] P.S. Bradley and U.M. Fayyad. Refining initial points for k-means clustering. In ICML, volume 98, pages 91–99, 1998.

[4] B.M. Briechle, Y. Kim, P. Ehrenreich, A. Erbe, D. Sysoiev, T. Huhn, U. Groth, and E. Scheer. Current-voltage characteristics of single-molecule diarylethene junctions measured with adjustable gold electrodes in solution. Beilstein Journal of Nanotechnology, 3:798–808, 2012. DOI: 10.3762/bjnano.3.89.

[5] M.J. Comstock, N. Levy, A. Kirakosian, J. Cho, F. Lauterwasser, J.H. Jarvey, D.A. Strubbe, J.M.J. Fréchet, D. Trauner, S.G. Louie, and M.F. Crommie. Reversible photomechanical switching of individual engineered molecules at a metallic surface. Physical Review Letters, 99:038301, 2007. DOI: 10.1103/PhysRevLett.99.038301.

[6] I.O. Contreras. Single-molecule conductance measurements: Correlations between chemical design and electronic properties. PhD thesis, TU Delft, 2018.

[7] J.C. Cuevas and E. Scheer. Molecular Electronics: An Introduction to Theory and Experiment. World Scientific Publishing, 2010.

[8] N. Darwish, A.C. Aragones, T. Darwisch, S. Ciampi, and I. Diez-Perez. Multi-responsive photo- and chemo-electrical single-molecule switches. Nano Letters, 14:7064–7070, 2014. DOI: 10.1021/nl50345999.

[9] E.W. Diau. A new trans-to-cis photoisomerization mechanism of azobenzene on the $s_1(n,\pi^*)$ surface. The Journal of Physical Chemistry, 108:9509–956, 2004. DOI: 10.1021/jp031149a.

[10] Dschwen. Single electron transistor. https://commons.wikimedia.org/wiki/File:Single_electron_transistor.svg, 2006. [Online; accessed Februari 5, 2018].

[11] D. Dulić, S.J. van der Molen, T. Kudernac, H.T. Jonkman, J.J.D. de Jong, and T.N. Bowden. One-way optoelectronic switching of photochromic molecules on gold. Physical review letters, 91:207402, 2003. DOI: 10.1103/PhysRevLett.91.207402.

[12] D. Dulić, T. Kuderac, A. Pužys, B.L. Feringa, and B.J. van Wees. Temperature gating of the ring-opening process in diarylethene molecular switches. Advanced Materials, 19:2898–2902, 2007. DOI: 10.1002/adma.200700161.

[13] R. Hayakawa, K. Higashiguchi, K. Matsuda, and T. Chikyow. Optically and electrically driven organic thin film transistors with diarylethene photochromic channel layers. Applied Materials and Interfaces, 5:3625–3630, 2013. DOI: 10.1021/am400030z.

[14] J. He, F. Chen, P.A. Liddell, J. Andréasson, S.D. Straight, D. Gust, T.A. Moore, A.L. Moore, J. Li, O.F. Sankey, and S.M. Lindsay. Switching of a photochromic molecule on gold electrodes: single-molecule measurements. Nanotechnology, 16:695–702, 2005. DOI: 10.1088/0957-4484/16/6/012.

[15] W. Hu, G. Zhang, S. Duan, Q. Fu, and Y. Luo. Molecular design to enhance the thermal stability of a photo swichable molecular junction based on dimethyldihydropyrene and cyclophanediene isomerization. The Journal of Physical Chemistry, 119:11468–11474, 2015. DOI: 10.1021/acs.jpcc.5b02201.

[16] C. Huang, M. Jevric, A. Borges, S.T. Olsen, J.M. Hamill, J. Zheng, Y. Yang, A. Rudnev, M. Baghernejad, P. Broekmann, A.U. Petersen, T. Wandlowski, K.V. Mikkelsen, G.C. SOlomon, M.B. Nielsen, and W. Hong. Single-molecule detection of dihydroazulene photo-thermal reaction using break junction technique. Nature Communications, 8, 2017. DOI: 10.1038/ncomms15436.

[17] M. Ikeda, N. Tanifuji, H. Yamaguchi, M. Irie, and K. Matsuda. Photoswitching of conductance of diarylethene-au nanoparticle network. Chemical Communications, 13:1355–1357, 2007. DOI: 10.1039/B617246F.

[18] C. Jia, A. Migliore, N. Xin, S. Huang, J. Wang, Q. Yang, S. Wang, H. Chen, D. Wang, B. Feng, Z. Liu, G. Zhang, D. Qu, H. Tian, M.A. Ratner, H.Q. Xu, A. Nitzan, and X. Guo. Covalently bonded single-molecule junctions with stable and reversible photoswitched conductivity. Science, 352:1443–1445, 2016. DOI: 10.1126science.aaf6298.

[19] V. Kaliginedi, A.V. Rudnex, P Moreno-Garcia, M. Bagdehernejad, C. Huang, W. Hong, and T. Wandlowski. Promising anchoring groupd for single-molecule conductance measurements. Royal Society of Chemistry, 16:23529–23539, 2014. DOI: 10.1039/C4CP03605K.

[20] N. Katsonis, T. Kudernac, M. Walko, S.J. van der Molen, B.J. van Wees, and B.L. Feringa. Reversible conductance switching of single diarylethenes on a gold surface. Advanced Materials, 18:1397–1400, 2006. DOI: 10.1002/adma.200600210.

[21] T. Kim, Z. Liu, C. Lee, J.B. Neaton, and L. Venkataraman. Charge transport and rectification in molecular junctions formed with carbon-based electrodes. Proceedings of the National Academy of Sciences, 111: 10928–10932, 2014. DOI: 10.1073.pnas.1406926111.

[22] Y. Kim, A. Garcia-Lekue, D. Sysoiev, T. Frederiksen, U. Groth, and E. Scheer. Charge transport in azobenzene-based single molecule junctions. American Physical Society, 109, 2012. DOI: 10.1103/PhycRevLett.109.26801.

[23] Y. Kim, T.J. Hellmuth, D. Sysoiev, F. Pauly, T. Pietsch, J. Wolf, A. Erbe, T. Huhn, U. Groth, U.E. Steiner, and E. Scheer. Charge transport characteristics fo diarylethene photoswitching single-molecule junctions. Nano Letters, 12:3736–3742, 2012. DOI: 10.1021/nl3015523.

[24] A.J. Kronemeijer, H.B. Akkerman, T. Kudernac, B.J. van Wees, B.L. Feringa, P.W.M. Blom, and B. de Boer. Reversible conductance switching in molecular devices. Advanced Materials, 20:1467–1473, 2008. DOI: 10.1002/adma.200800053.

[25] A.S. Kumar, T. Ye, T. Takami, B. Yu, A.K. Flatt, J.M. Tour, and P.S. Weiss. Reversible photo-switching of single azobenzene molecules in controlled nanoscale environments. Nano Letters, 8:1644–1648, 2008. DOI: 10.1021/nl080323+.

[26] K.E. Lee, J.U. Lee, D.G. Seong, M. Um, and W. Lee. Highly sensitive ultraviolet light sensor based on photoactive organic gate dielectrics with an azobenzene derivative. Journal of Physical Chemistry, 120: 23172–23179, 2016. DOI: 10.1021/acs.jpcc.6b08427.

[27] S. Lenfant, Y. viero, C. Krzeminski, D. Vuillame, D. Demeter, I. DOrba, M. Ocafrain, P. Blanchard, J. ROncali, C. van Dyk, and J. Cornil. New photomechanical molecular switch based on a linear pi-conjugated system. Journal of Physical Chemistry, 121:12416–12425, 2017. DOI: 10.1021/acs.jpcc.7b01240.

[28] Z. Li, L. Liao, W. Sun, C. Xu, C. Zhang, C. Fang, and C. Yan. Reconfigurable cascade circuit in a photo- and chemical-switchable fluorescent diarylethene derivative. The Journal of Physical Chemistry, 112: 5190–5196, 2008. DOI: 10.1021/jp711613y.

[29] C.A. Martin, R.H. Smit, R. van Egmond, H.S.J. van der Zant, and J.M. Ruitenbeek. A versatile low-temperature setup for the electrical characterization of single-molecule junctions. Review of Scientific Instruments, 82, 2011. DOI: 10.1063/1.3593100.

[30] J.M. Mativetski, G. Pace, M. Elbing, M.A. Rampi, M. Mayor, and P. Samori. Azobenzenes as light-controlled molecular electronic switches in nanoscale metal-molecule-metal junctions. Journal of American Chemical Society, 130:9192–9193, 2008. DOI: 10.1021/ja8018093.

[31] K. Matsuda, H. Yamaguchi, T. Sakano, M. Ikeda, N. Tanifuji, and M. Irie. Conductance photoswitching of diarylethene-gold nanoparticle network induced by photochromic reaction. Journal of Physical Chemistry, 112:17005–17010, 2008. DOI: 10.1021/jp807479g.

[32] F. Meng, Y. Hervailt, L. Norel, K. Costuas, C. van Dyck, V. Geskin, J. Cornil, H.H. Hng, S. Rigaut, and X. Chen. Photo-modulable molecular transport junctions based on organometallic molecular wires. Chemical Science, 3:3113–3118, 2012. DOI: 12.1039/c2sc20323e.

[33] Y. Nazarov and Y. Blanter. Quantum Transport: Introduction to Nanoscience. Cambridge University Press, 2009.

[34] M.L. Perrin. Charge Transport Through Single-Molecule Junctions: Experiments and Theory. PhD thesis, TU Delft, 2015.

[35] G. Reecht, C. Lotze, D. Sysoiev, T. Huhn, and K.J. Franke. Visualizing the role of molecular orbitals in charge transport through individual diarylethene isomers. Nano, 10:10555–10562, 2016. DOI: 10.1021/acsnano.6b06559.

[36] C. Reese, M. Roberts, M. Ling, and Z. Bao. Organic thin film transistors. Materials today, 7:20–27, 2004. DOI: 10.1016/S1369-7021(04)00398-0.

[37] D. Roldan, V. Kaliginedi, S. Cobo, V. Kolivoska, C. Bucher, W. Hong, G. Royal, and T. Wandlowski. Charge transport in photoswitchable dimethyldihydropyrene-type single-molecule junctions. The Journal of American Chemical Society, 135:5974–5977, 2013. DOI: 10.1021/ja401484j.

[38] C. Sciascia, R. Castagna, M. Dekermanjian, R. Martel, A.R.S. Kandada, F. Di Fonzo, A. Bianco, C. Bertarelli, M. Meneghetti, and G. Lanzani. Light-controlled resistance modulation in a photochromic diarylethene-carbon nanotube blend. The Journal of Physical Chemistry, 116:19483–19489, 2012. DOI: 10.1021/jp212231j.

[39] G. Sedgi, K. Sawada, L.J. Esdaile, M. Hoffman, H.L. Anderson, D. Bethell, W. Hais, S.J. Higgins, and R.J. Nichols. Single molecule conductance of porphyrin wires with ultralow attenuation. American Chemical Society, 130:8582–8583, 2008. DOI: 10.1021/ja802281c.

[40] S. Seo, M. Min, S.M. Lee, and H. Lee. Photo-switchable molecular monolayer anchored between highly transparent and flexible graphene electrodes. Nature Communications, 4, 2013. DOI: 10.1038/ncomms2937.

[41] Su-No-G. Azobenzene isomerization. https://commons.wikimedia.org/wiki/File:Azobenzene_isomerization.png, 2007. [Online; accessed Februari 5, 2018].

[42] E.S. Tam, J.J. Parks, W.W. Shum, Y. Zhong, M.B. Satiago-Berrios, X. Zheng, W. Yang, G.K.L. Chan, H.D. Abruna, and D.C. Ralph. Single-molecule conductance of pyridine-teminated dithienylethene switch molecules. Nano, 5:5115–5123, 2011. DOI: 10.1021/nn201199b.

[43] B.E. Tebikachew, H.B. Li, A. Pirotta, K. Borjesson, G.C. Solomon, J. Hihath, and K. Moth-Poulsen. Effect of ring strain on the charge transport of a robust norbornadiene-quadricyclane-based molecular photoswitch. Journal of Physical Chemistry, 121:7094–7100, 2017. DOI: 10.1021/acs.jpcc.7b00319.

[44] J.M. Thijssen and H.S.J. van der Zant. Charge transport and single electron effects in nanoscale systems. Physica Status Solidi, 245, 2008. DOI: 10.1002/pssb.200743470.

[45] T. Toyama, K. Higashigushi, T. Nakamura, H. Yamaguchi, E. Kusaka, and K. Matsuda. Photoswitching of conductance of diarylethene-gold nanoparticle network based on the alteration of π-conjugation. The Journal of Physical Chemistry, 7:2113–2118, 2016. DOI: 10.1021/acs.jpclett.6b00993.

[46] K. Uchida, Y. Yamanoi, T. Yonezawa, and H. Nishihara. Reversible on/off conductance switching of a single diarylethene immobilized on a silicon surface. Journal of the American Chemical Society, 133: 9239–9241, 2011. DOI: 10.1021/ja203269t.

[47] H. Valkenier, E.H. Huisman, P.A. van Hal, D.M. de Leeuw, R.C. Chiechi, and J.C. Hummelen. Formation of high-quality self-assembled monolayers of conjugated dithiols on gold: Base matters. American Chemical Society, 133:4930–4939, 2011. DOI: 10.1021/ja110358t.

[48] M. Del Valle, R. Gutierrez, C. Tejedor, and G. Cuniberti. Tuning the conductance of a molecular switch. Nature Nanotechnology, 2:176–179, 2007. DOI: 10.1038/nnano.2007.38.

[49] S.J. van de Molen, J. Liao, T. Kuderac, J.S. Agustsson, L. Bernard, M. Calame, B.J. van Wees, B.L. Feringa, and C. Schonenberger. Light-controlled conductive switching of ordered metal-molecule-metal devices. Nano Letters, 9(1):76–80, 2008. DOI: 10.1021/nl802487j.

[50] S.J. van der Molen and P. Liljeroth. Charge transport through molecular switches. Journal of Physics: Condensed Matter, 22, 2010. DOI: 10.1088/0953-8984/22/13/133001.

[51] A.C. Whalley, M.L. Steigerwald, X. Guo, and C. Nuckolls. Reversible switching in molecular electronic devices. Journal of the American Chemical Society, 129:12590–12591, 2007. DOI: 10.1021/ja073127y.

[52] I'm with gerrit. Dithienylethene. https://commons.wikimedia.org/wiki/File:Dithienylethene.png, 2007. [Online; accessed Februari 5, 2018].

[53] N. Xin, C. Jia, J. Wang, S. Wang, M. Li, Y. Gong, G. Zhang, D. Zhu, and X. Guo. Thermally activated tunneling transition in a photoswitchable single-molecule electrical junction. The Journal of physical Chemistry, 8:2849–2854, 2017. DOI: 10.1021/asc.jpclett.7b01063.

[54] A.I. Yanson, G.R. Bollinger, H.E. van den Brom, N. Agrait, and J.M. van Ruitenbeek. Formation and manipulation of a metallic wire of single gold atoms. Nature, 395:783–785, 1998. DOI: 10.1038/27405.